Aspects of Nanophotonics: Radiative Cooling, Image Processing and Topology

Presented by:

OSA Nanophotonics Technical Group

OSA

Nanophotonics Technical Group

About the OSA Nanophotonics Technical Group

Mission statement

OSA Nanophotonics Technical Group focuses on the study and design of optics and optical devices that interact with light on the nanometer scale.

Group Chair

Cheng Zhang

National Institute of Standards & Technology (NIST), USA

cheng.zhang@nist.gov

Social Media Officer

Sachin Kumar Srivastava

Indian Institute of Technology Roorkee, India

achinchitransh@gmail.com

Create a community for nanophotonic researchers

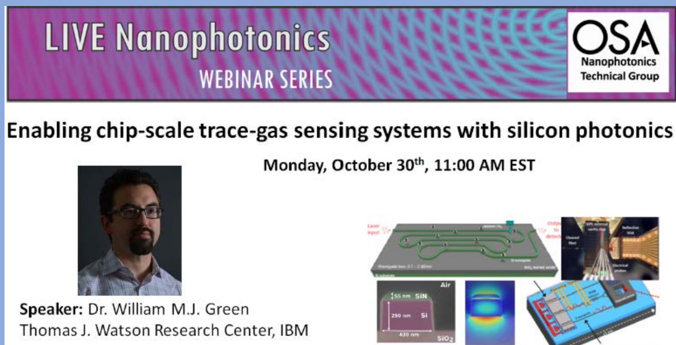

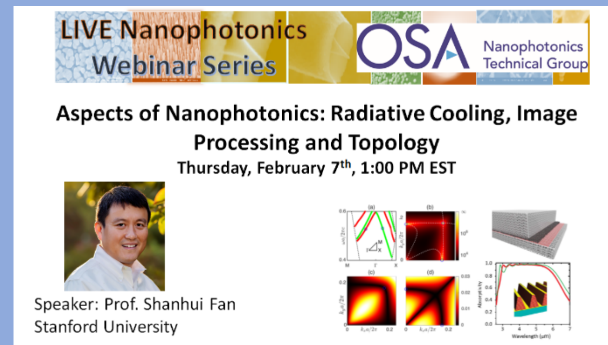

Webinars

20 x 20 Talks at CLEO

Personalized mentoring at FiO

Special events at OSA conferences

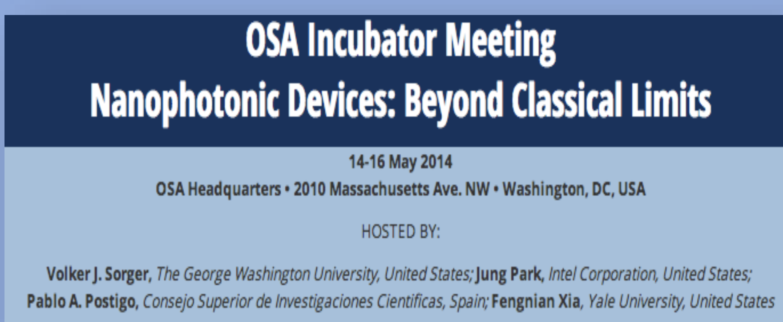

Incubator meetings

Where to find us ?

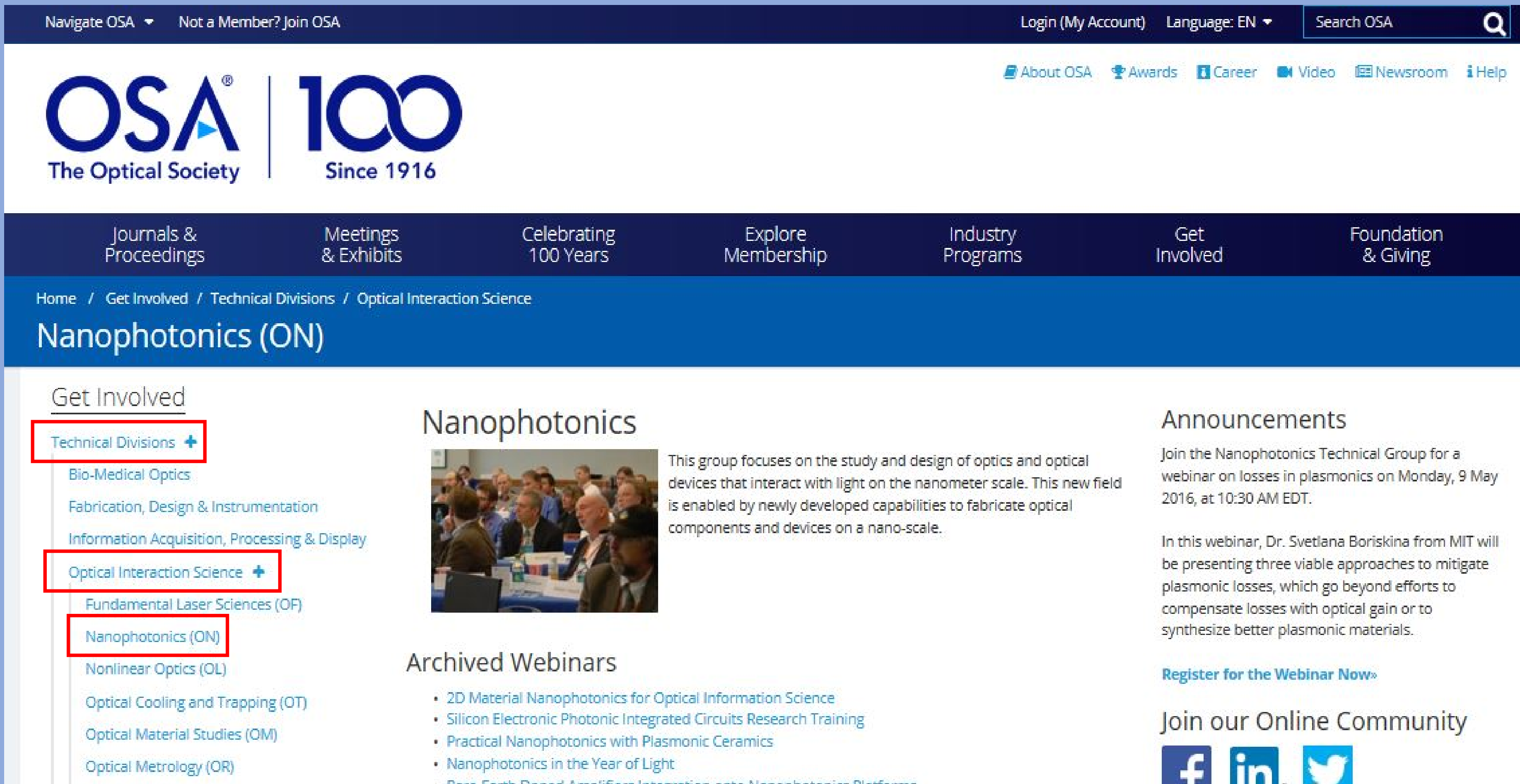

Website: www.osa.org/NanophotonicsTG

Email: osananophotonics@gmail.com

Where to find us ?

@Nano_OSA

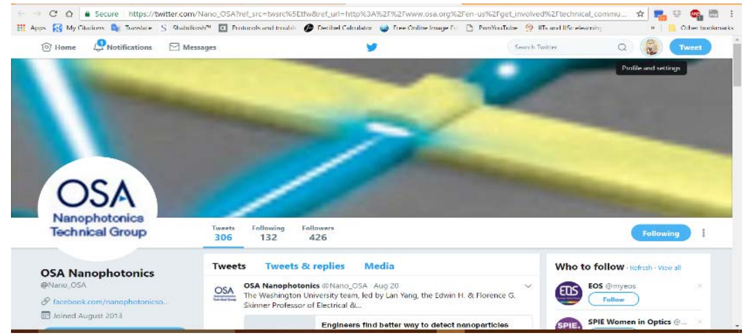

facebook.com/nanophotonicsosa

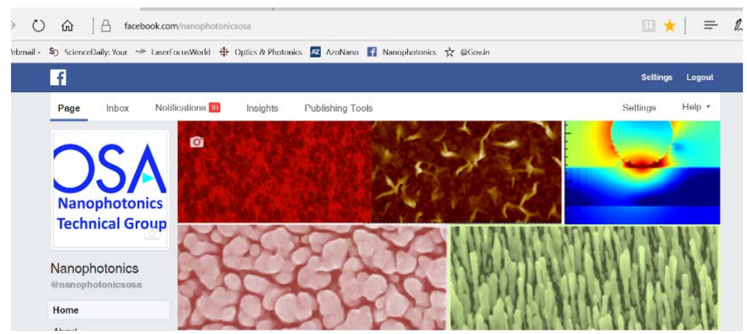

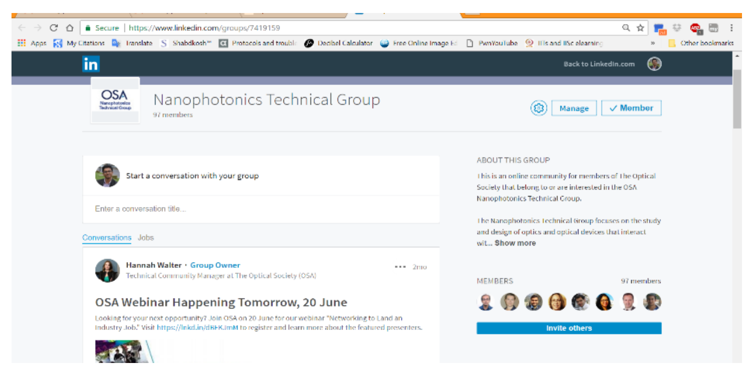

Past Chairs and Executive Team (2016-2018)

Peter B. Catrysse

Stanford Univ., USA
pcatryss@stanford.edu

Jincy Jose

OPTIS NA, USA
jincyjosemail@gmail.com

Pablo Aitor Postigo

CSIC, Spain
pabloaitor.postigo@imm.cnm.csic.es

Nadir Dagli

UCSB, USA
dagli@ece.ucsb.edu

Lin Zhang

Tianjin Univ., China
lin_zhang@tju.edu.cn

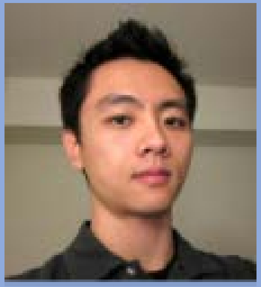

Jung S. Park

Intel, USA
jung.s.park@intel.com

Aspects of nanophotonics: radiative cooling, image processing, and topology

Shanhui Fan
Department of Electrical Engineering
Ginzton Laboratory
Stanford University

Outline

Energy technology

Information technology

Fundamental aspects

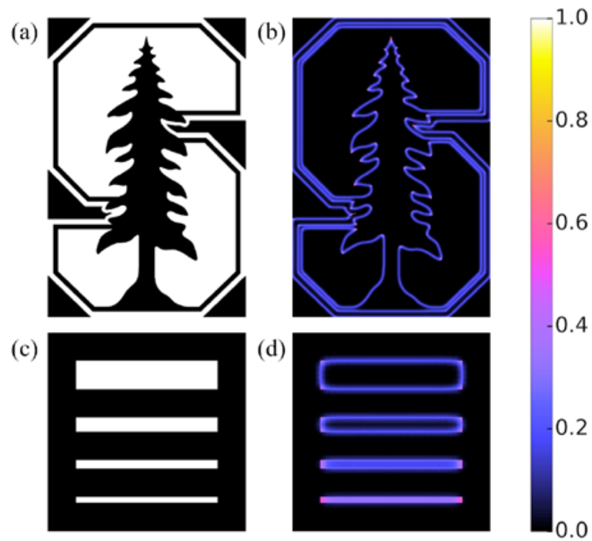

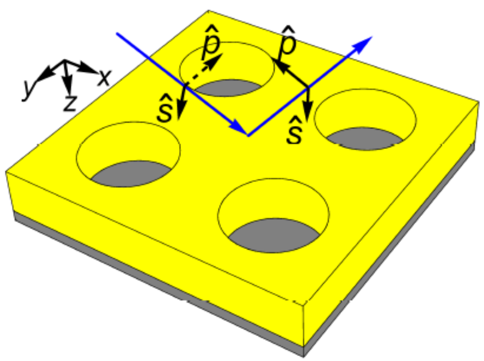

Radiative cooling

Image processing

Topology

Blackbody radiation

~3000K

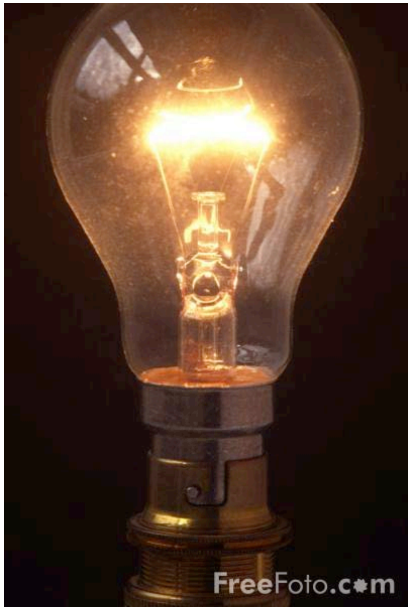

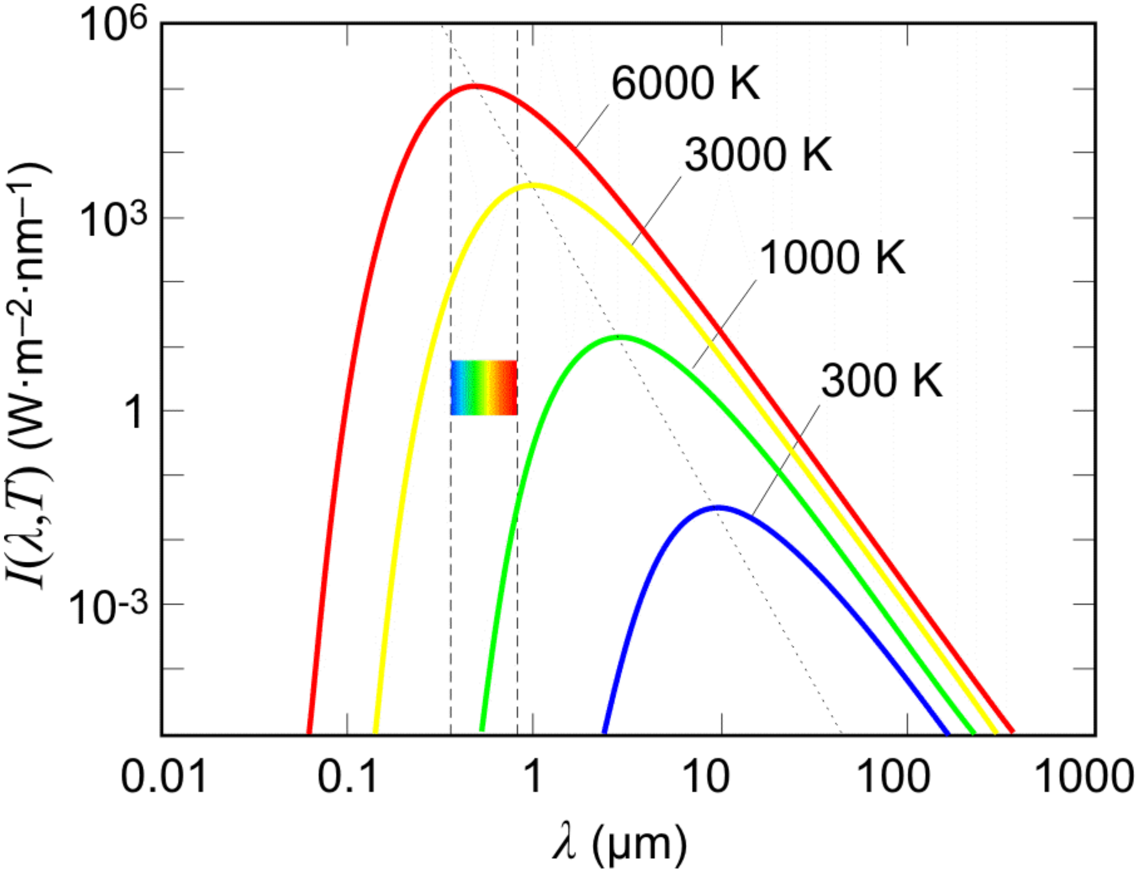

Conventional thermal radiator: broad-band, all angle emission

Narrow-band thermal radiation from gold antenna

$w = 0.4\mu m, l = 1.7\mu m$

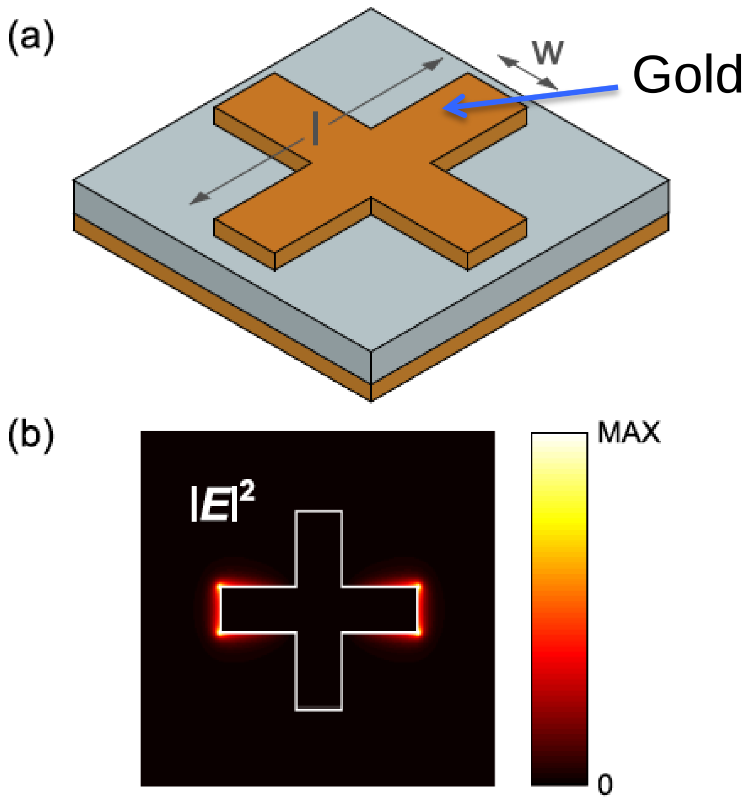

L. Zhu et al, APL 102, 103104 (2013)

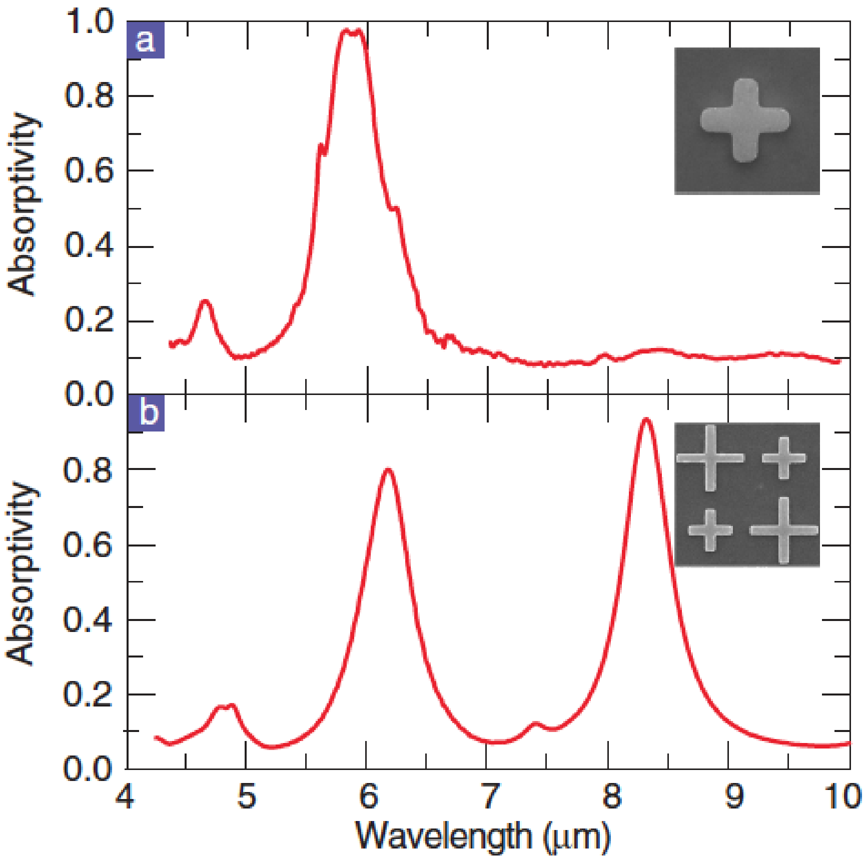

X. Liu et al, PRL 107, 045901 (2011)

For a review of nanophotonic control of thermal radiation see:
S. Fan, Joule, 1, 264-273 (2017)

Harvesting The Coldness of the Universe

Sun ~ 6000K

Universe
~ 3K

Earth ~300K

Carnot
efficiency
limit

$$\eta = 1 - \frac{T_L}{T_H}$$

We do have radiative access to the outer space

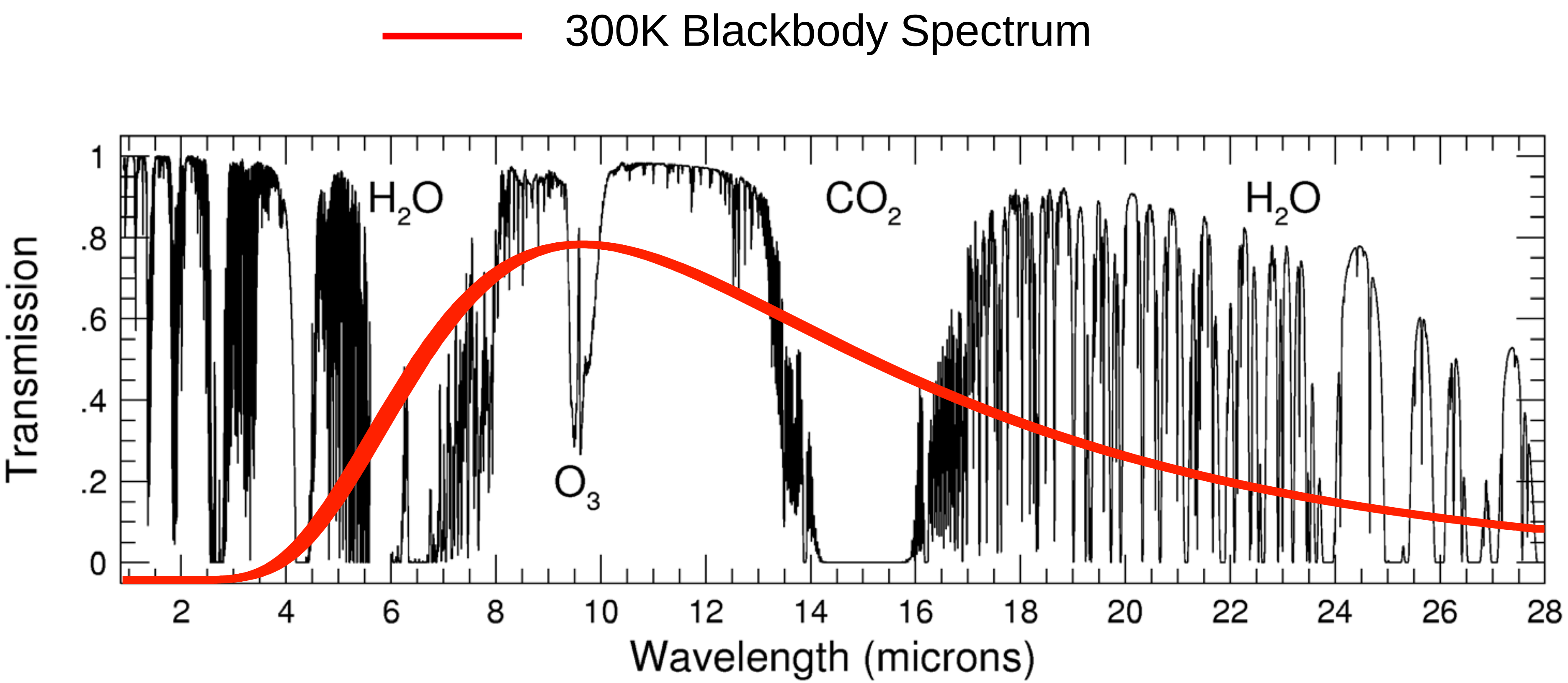

http://www.astronomy.ohio-state.edu/~pogge/Ast161/Unit5/atmos.html

Night-time radiative cooling

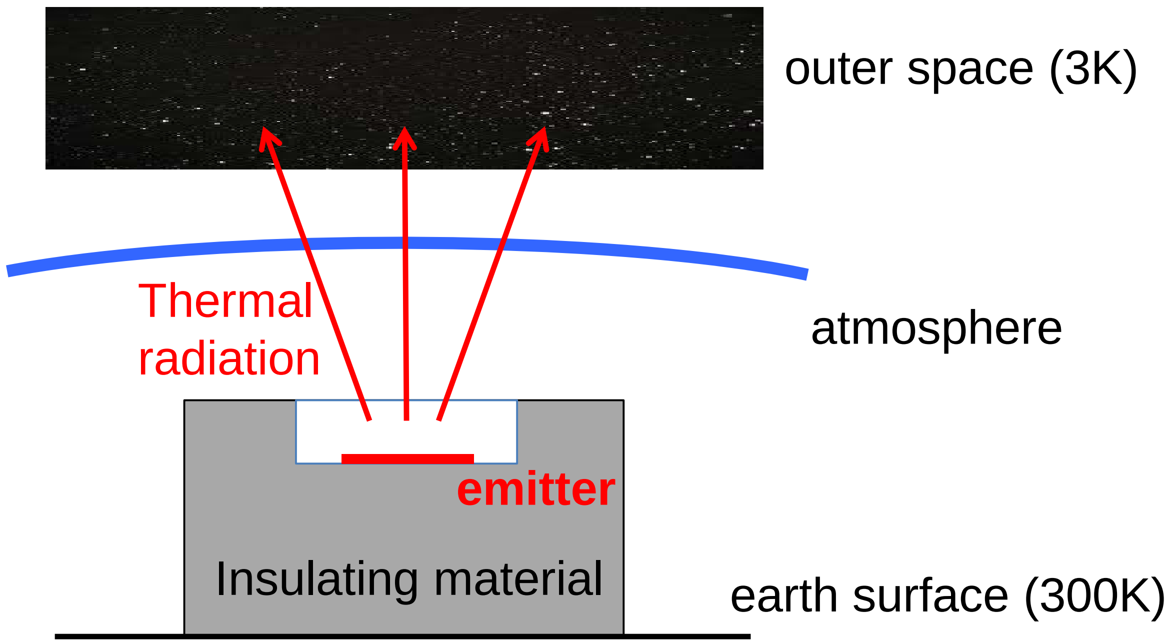

- Requires a good blackbody emitter.
- Cool to a temperature that is 13C below ambient.
- Limited use of night-time cooling.

C. G. Granqvist and A. Hjortsberg, Journal of Applied Physics 52, 4205 (1981).
A. R. Gentle and G. B. Smith, Nano Letters 10, 373 (2010).

Daytime radiative cooling

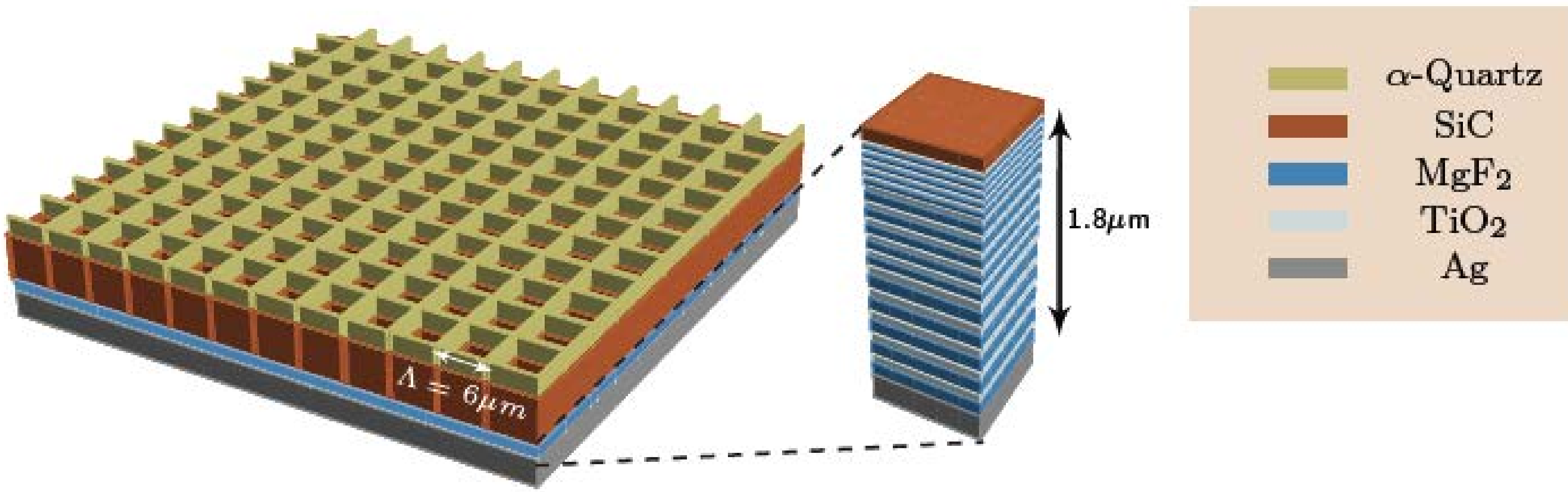

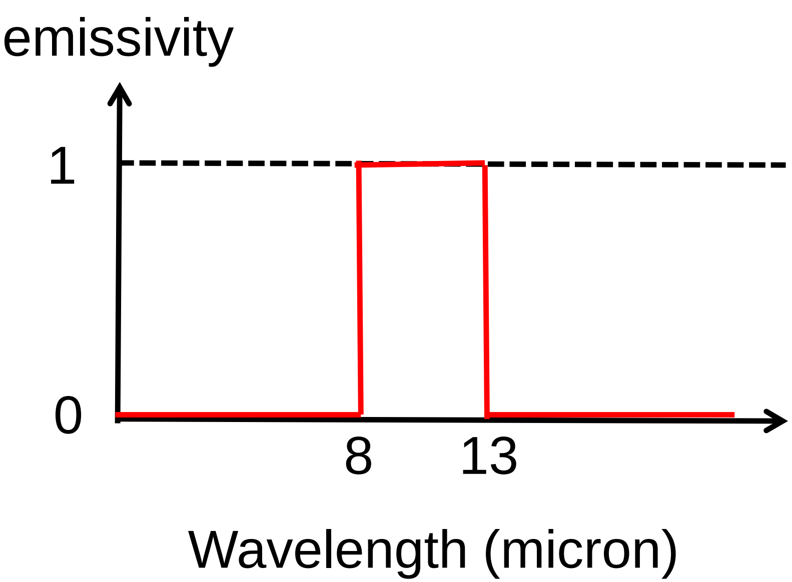

- A mirror in the solar wavelength range.
- "Black" in the 8-13 micron window.
- Sub-freezing temperature under the sun.
- Cooling power exceeding $100 W/m^2$.

E. Rephaeli, A. Raman and S. Fan, Nano Letters 13, 1451 (2013).

Stanford daytime radiative cooling experiment

Sample: 8 inch wafer

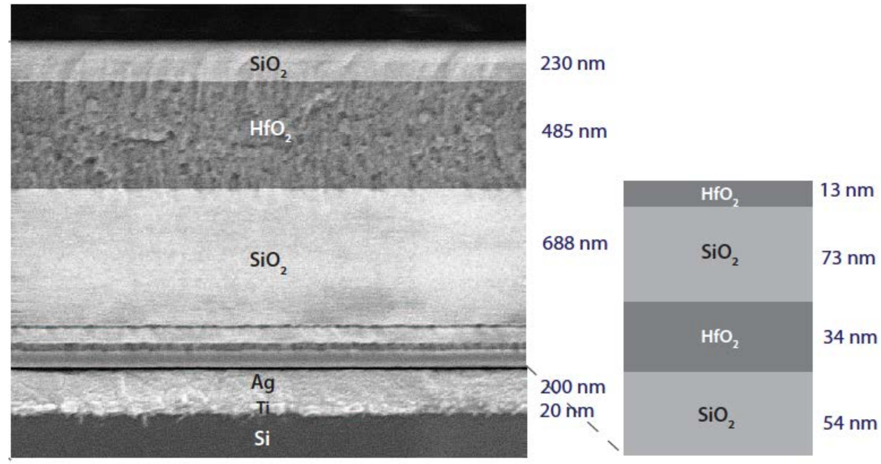

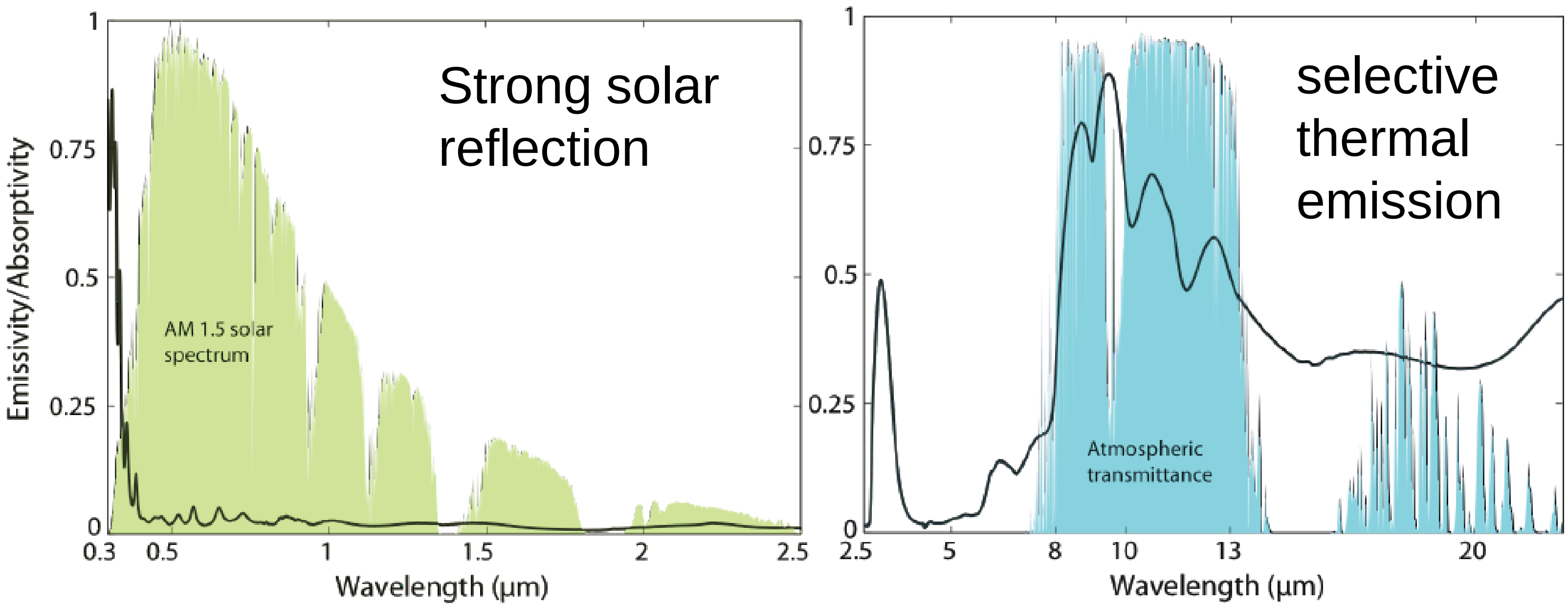

A. Raman, M. Anoma, L. Zhu, E. Rephaeli, and S. Fan, Nature 515, 540 (2014).

Rooftop Setup

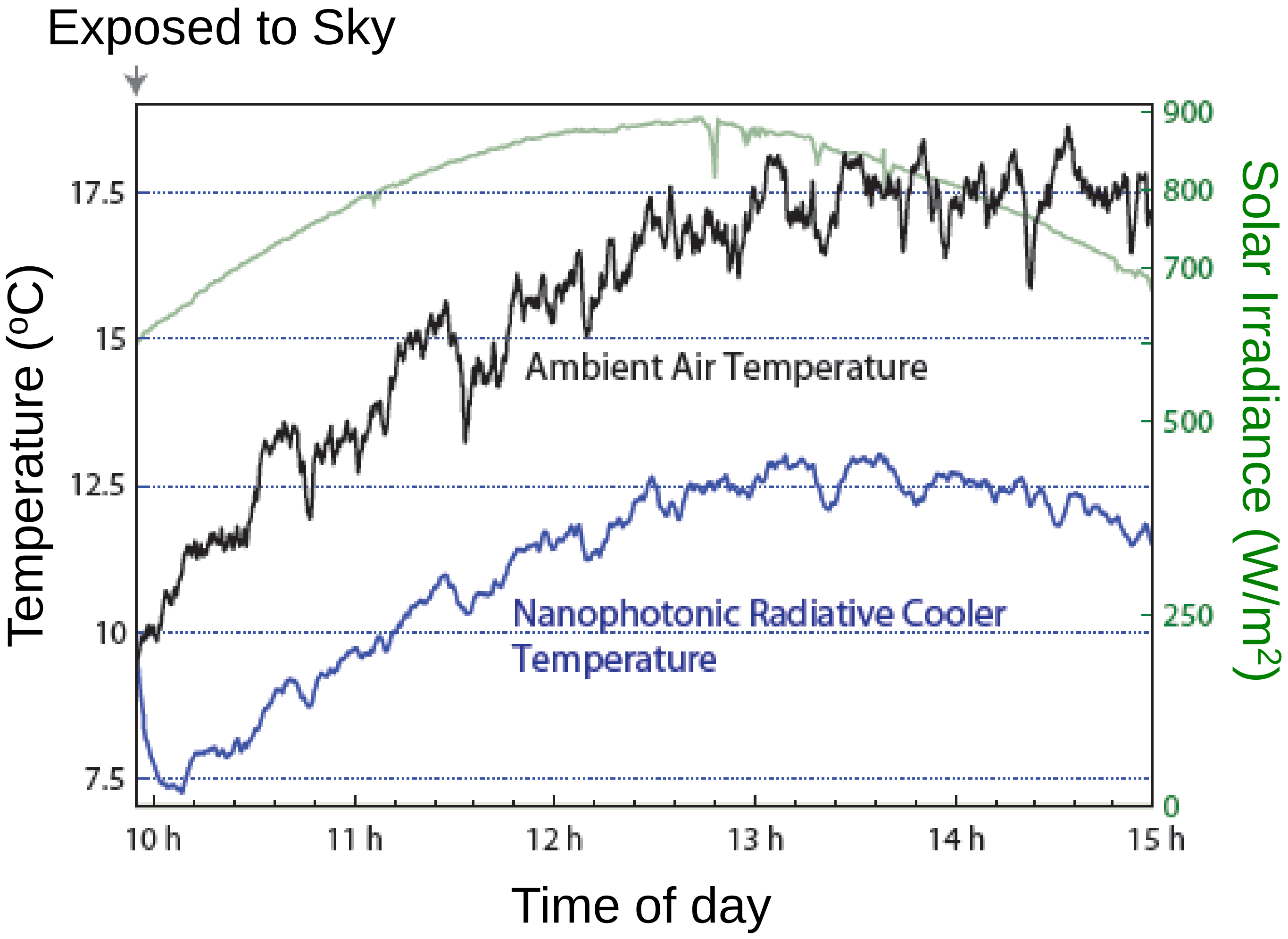

A. Raman, M. Anoma, L. Zhu, E. Rephaeli, and S. Fan, Nature 515, 540 (2014).

Cooling Power Measurement

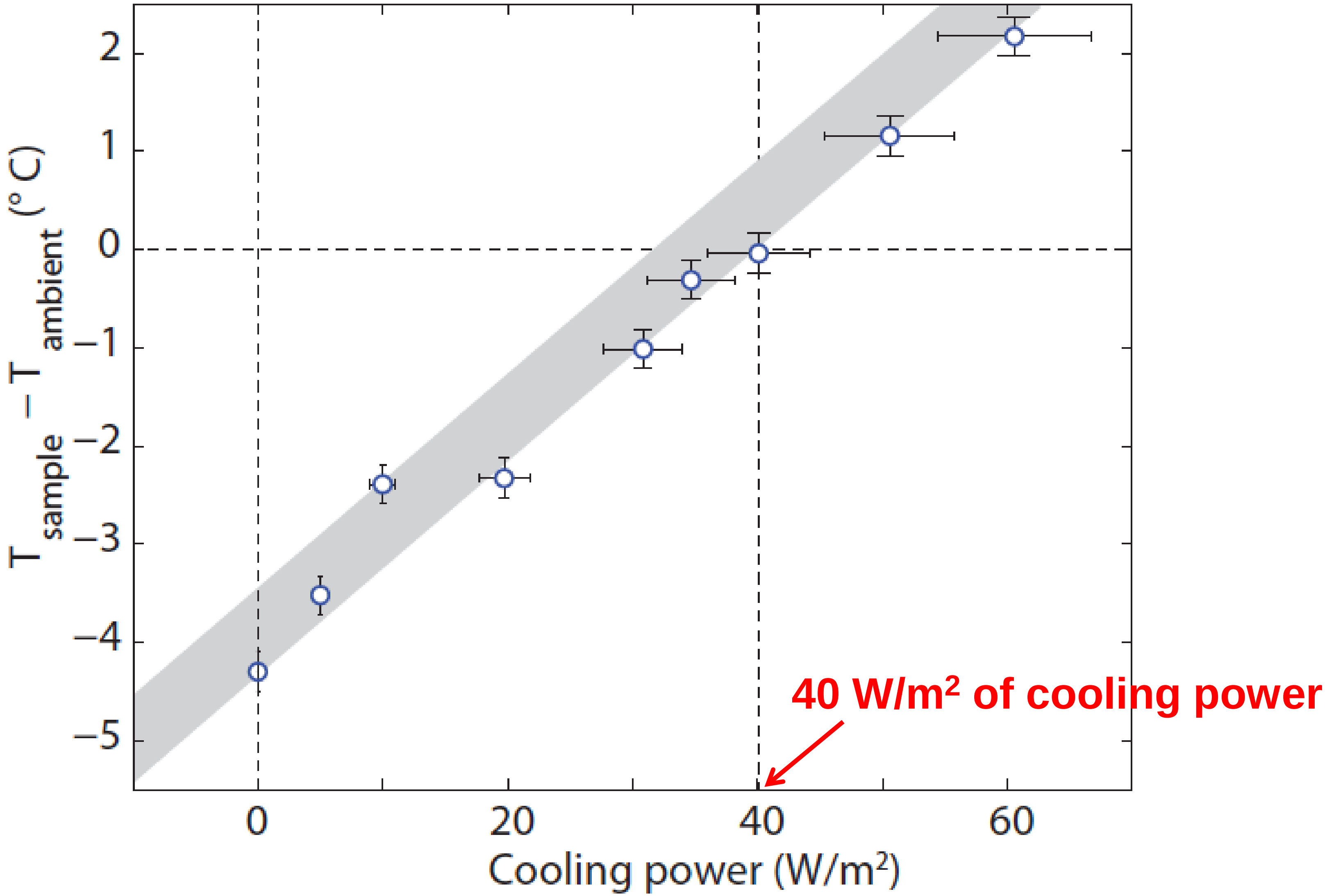

Theoretical limit exceeds 100 W/m^2

Subsequent daytime radiative cooling experiments

N. Shi, N. Yu and R. Wehner et al, Science (2015)

J. Kou, S. Fan, A. Minnich et al, ACS Photonics (2017)

Y. Zhai, R. Yang, and X. Yin et al, Science (2017)

System demonstration: close-loop water cooling

15% of US power consumption
goes to air-conditioning

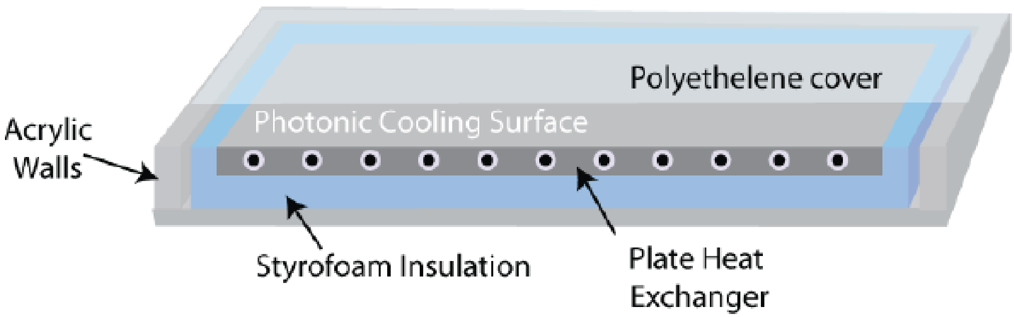

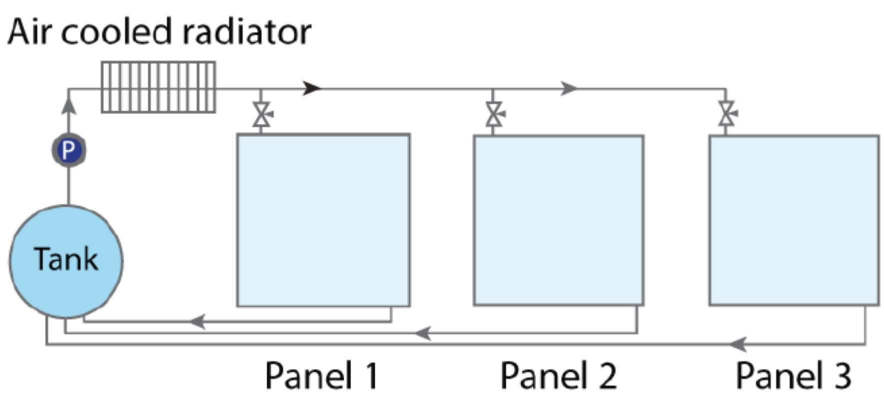

Water flow rate: 0 0.12 0.29L/min/m^2

Each module has of $0.37m^2$ of cooling area

E. Goldstein, A. Raman and S. Fan, Nature Energy 2, 17413 (2017).

Ideally, one can get 3K

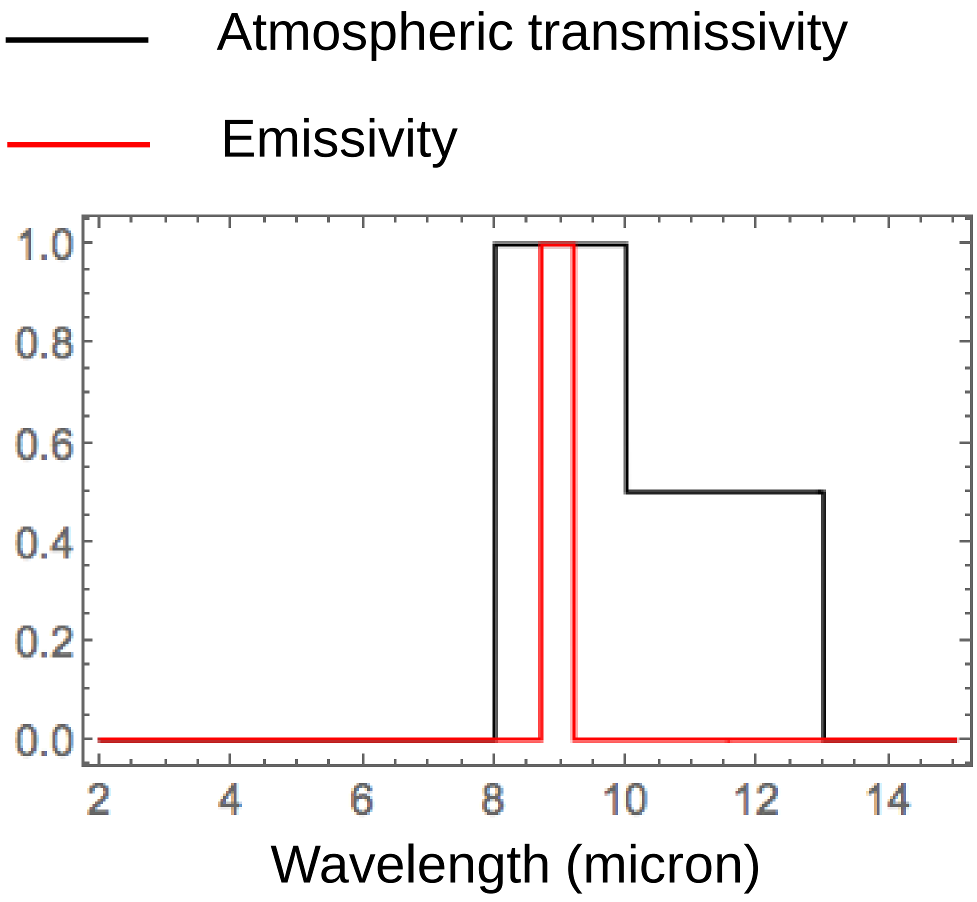

If the atmosphere has a wavelength range that is perfectly transmitting, with a selective emitter one should be able to reach 3K.

Very low temperature can be achieved with selective emitter

Transmission at Stanford
(dew point -1°C.)

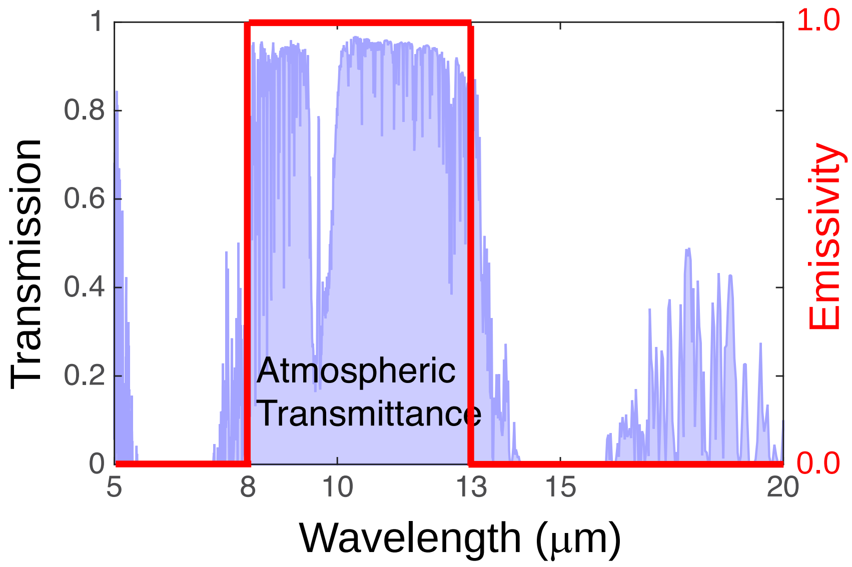

Assumes no parasitic heat load

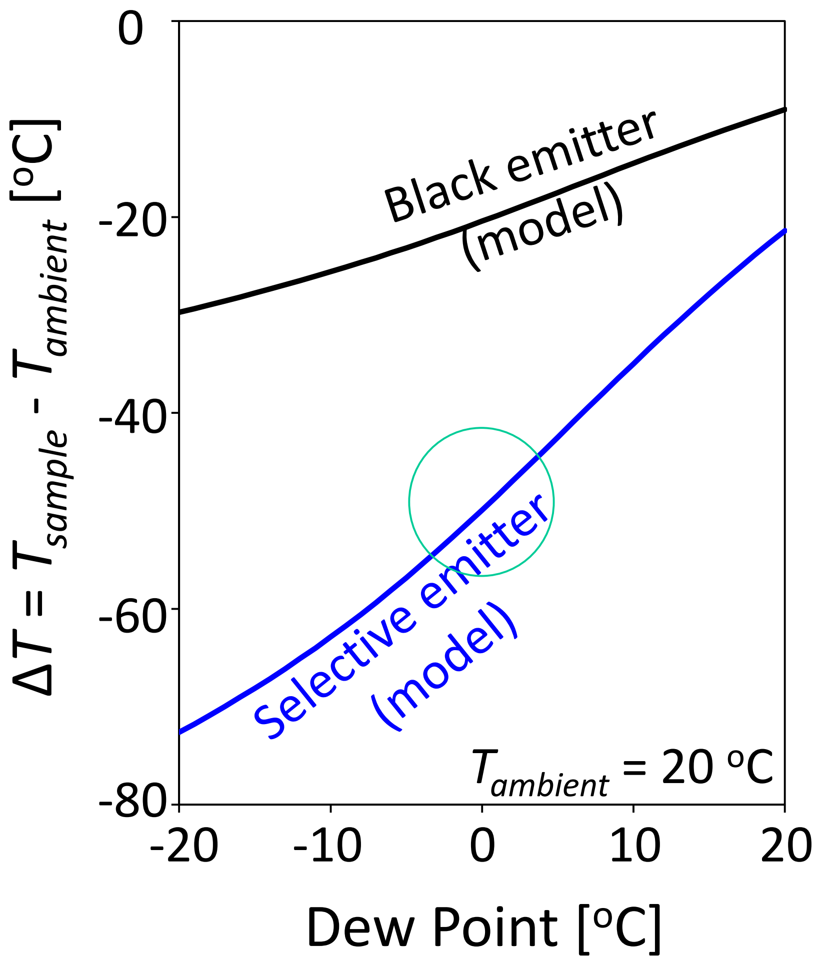

E. Rephaeli, A. Raman, and S. Fan, Nano Letters 13, 1451 (2013)

Towards Fundamental Limit of Radiative Cooling

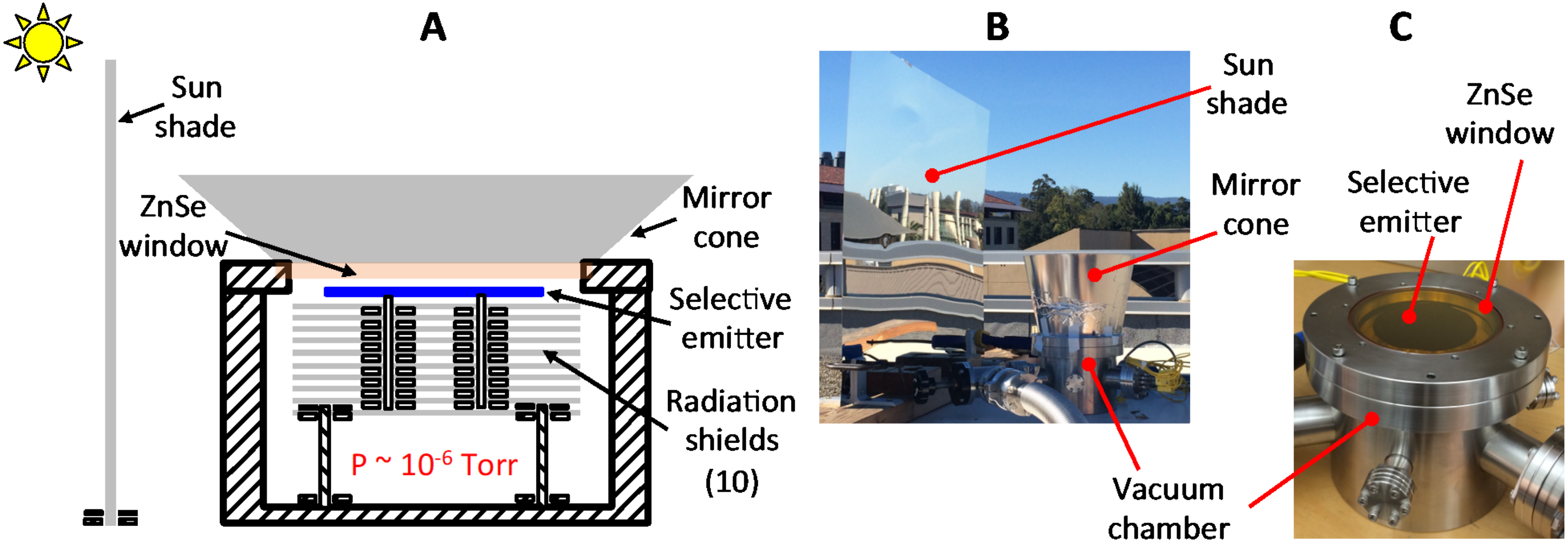

Z. Chen, L. Zhu, A. Raman, and S. Fan, Nature Communications 7, 13729 (2016)

Ultra-High Performance Continuous Radiative Cooling Over Day and Night

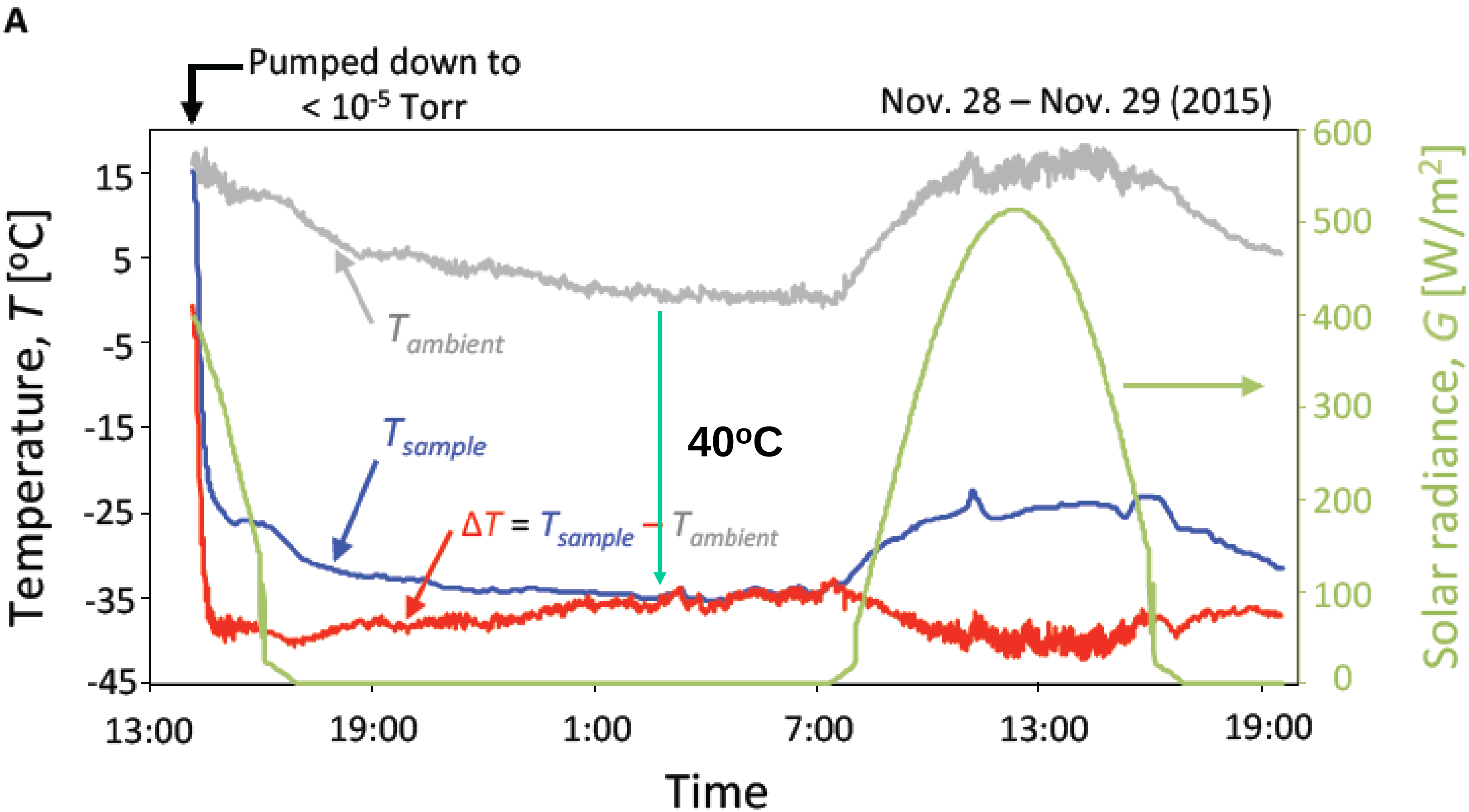

Z. Chen, L. Zhu, A. Raman, and S. Fan, Nature Communications 7, 13729 (2016).

Simultaneous solar energy harvesting and radiative cooling

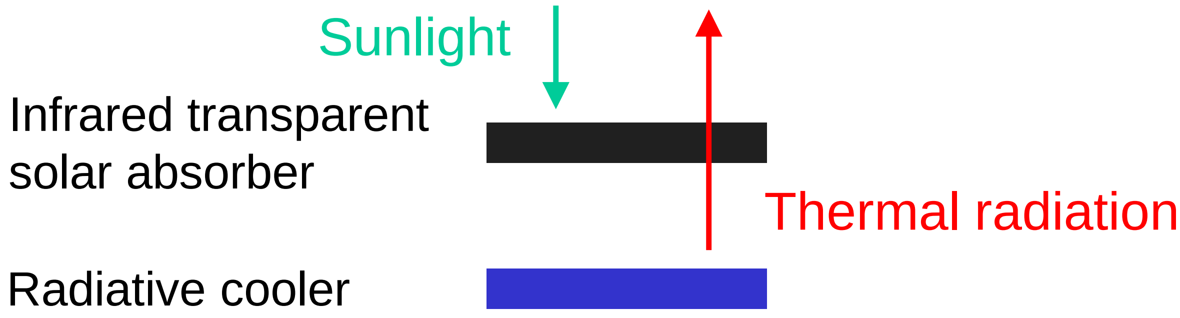

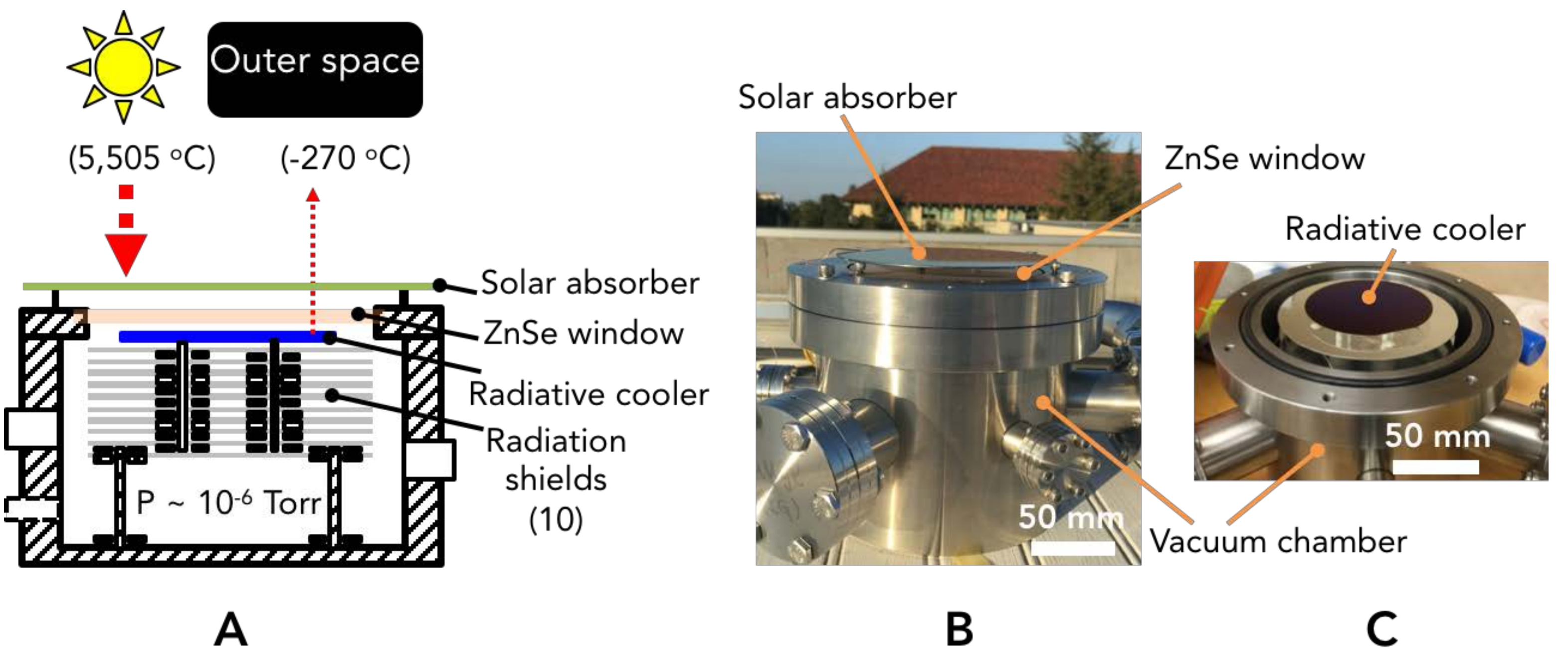

Z. Chen, L. Zhu, W. Li, and S. Fan, Joule, vol. 3, pp. 101-110 (2019)

Simultaneous solar energy harvesting and radiative cooling

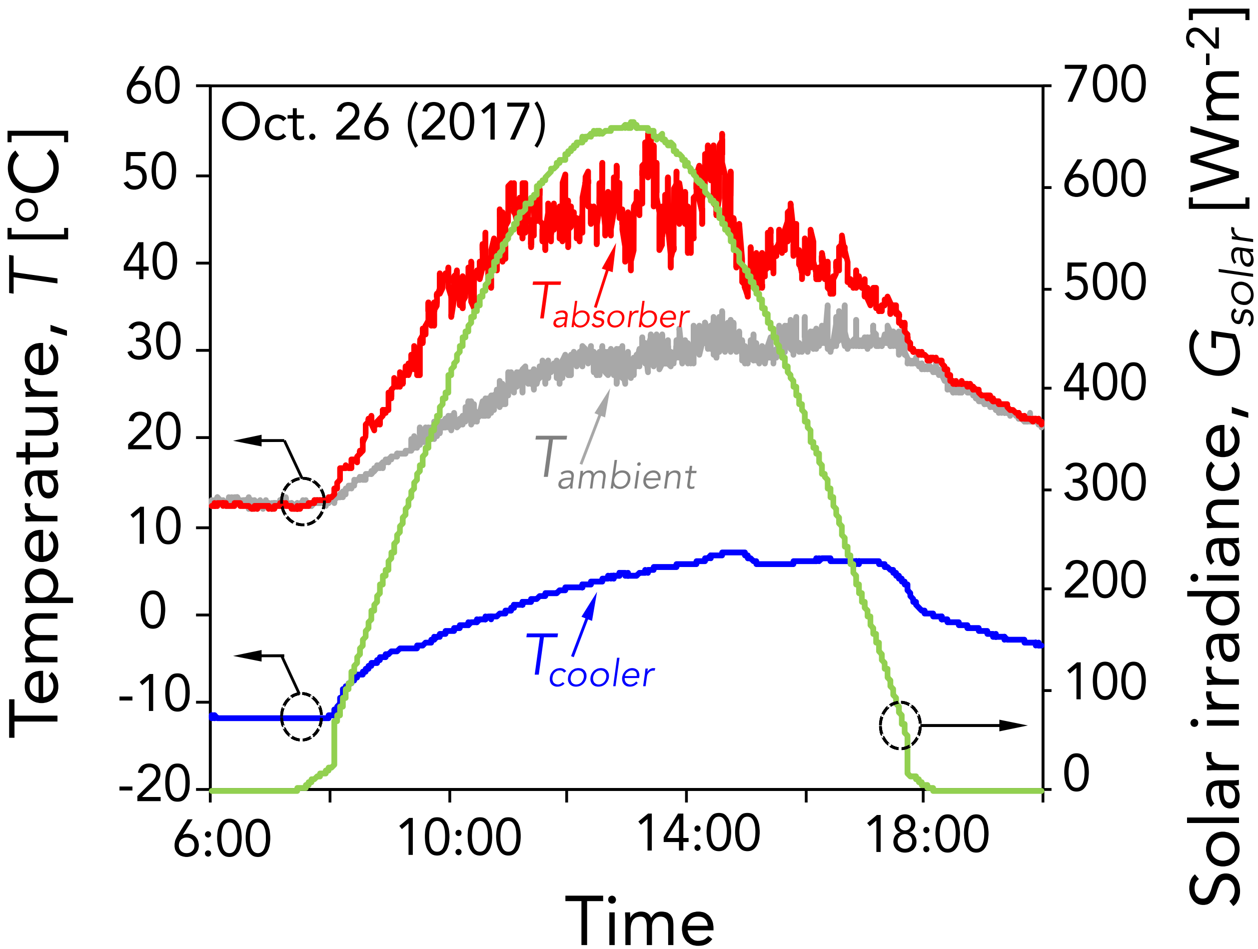

Z. Chen, L. Zhu, W. Li, and S. Fan, Joule, vol. 3, pp. 101-110 (2019)

Control the thermal load of a colored object

Combine radiative cooling with the utilization of sunlight

L. Zhu, A. Raman and S. Fan, Applied Physics Letters 103, 223902 (2013).

Radiative thermal load

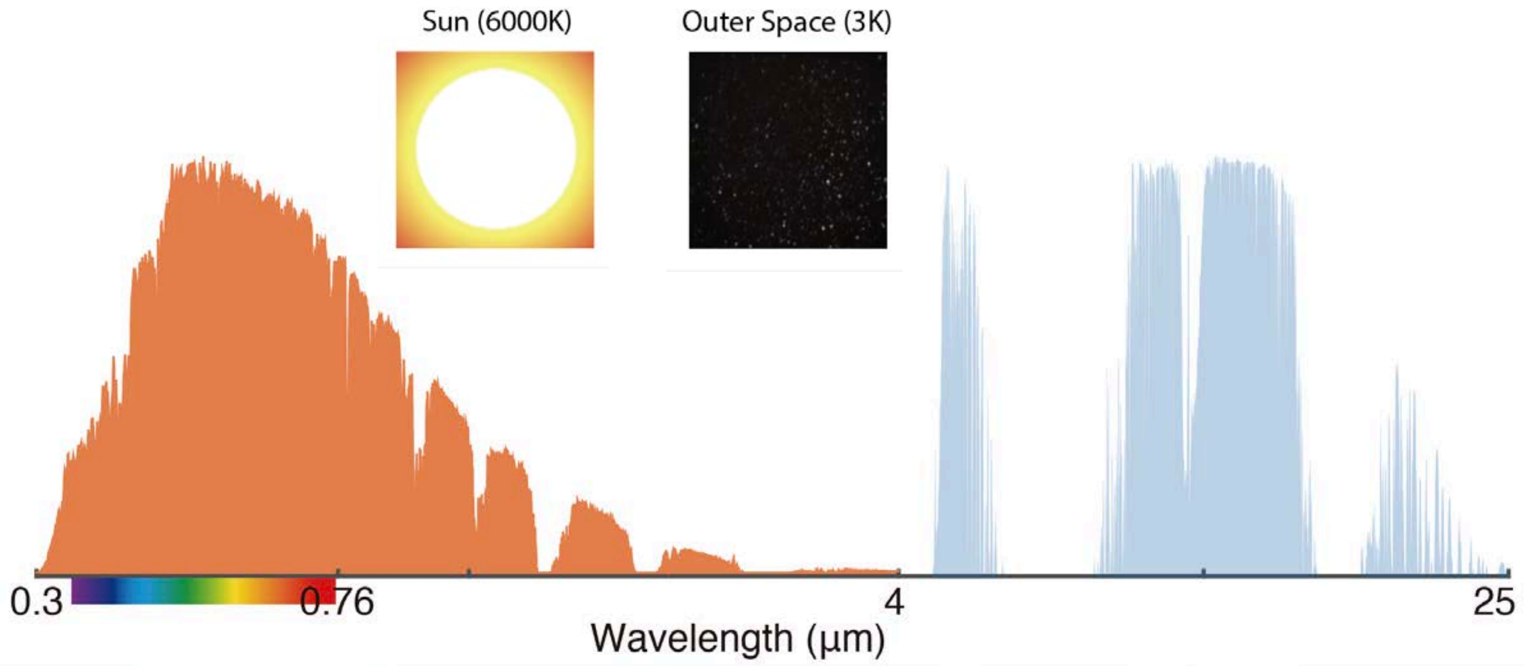

Radiative thermal load – radiative cooling

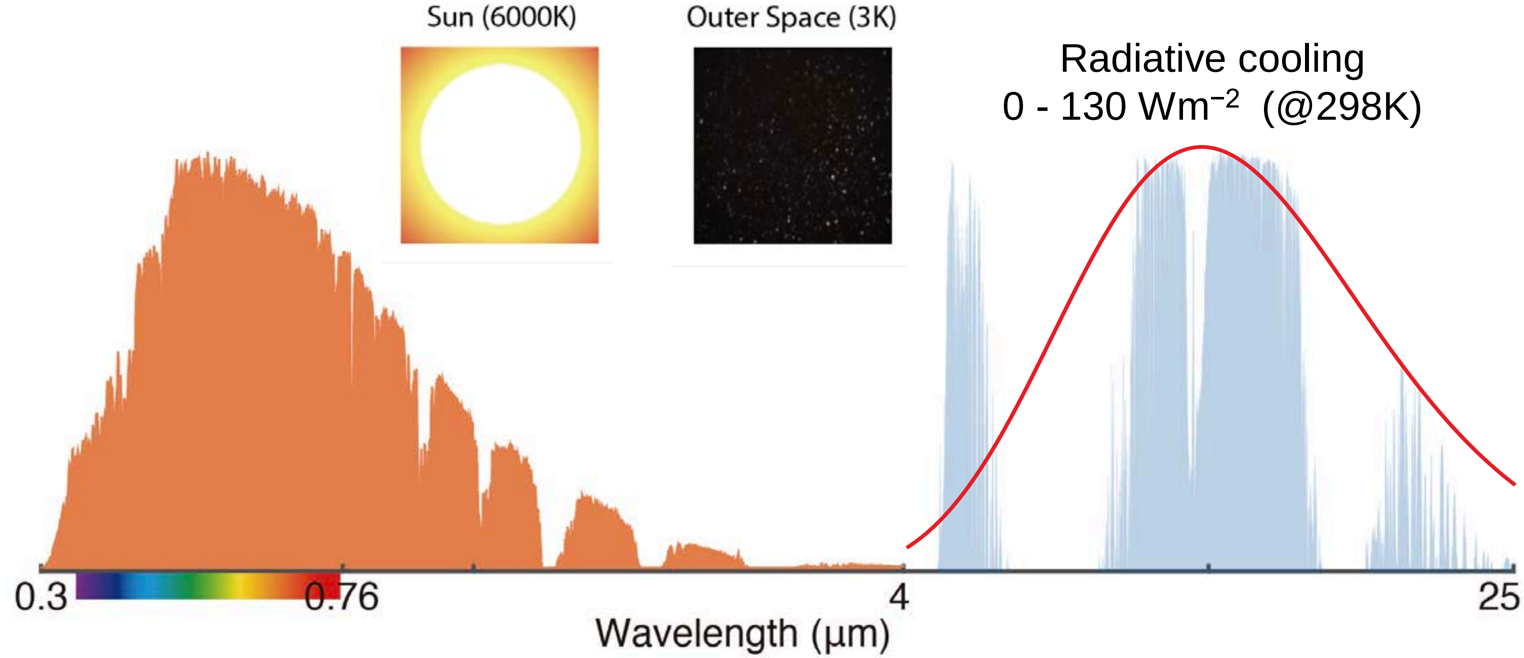

Zhu, L., Fan, S. *APL* (2013).

Radiative thermal load – near infrared

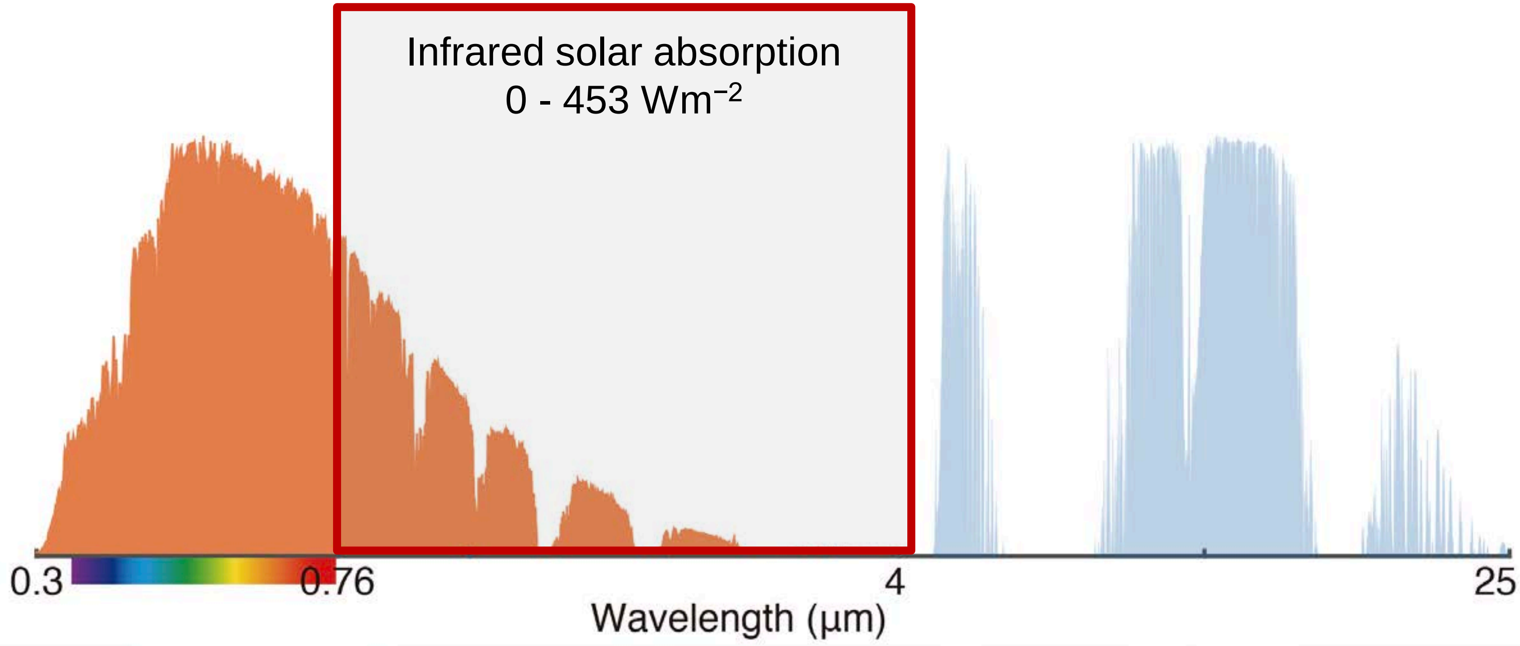

Smith, G. B., Gentle, A. R. *Solar Energy Materials and Solar Cells* (2003).

Synnefa, A., Santamouris, M. & Apostolakis, K. *Sol. Energy* (2007).

Radiative thermal load - visible

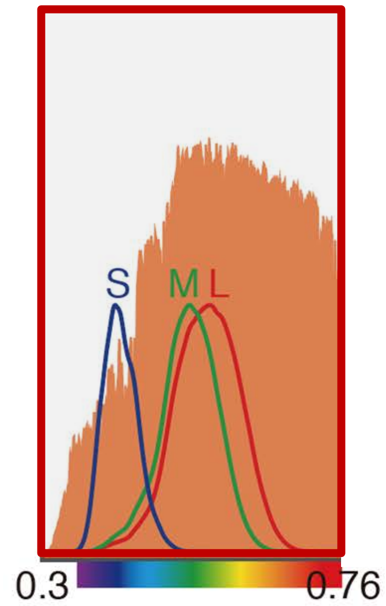

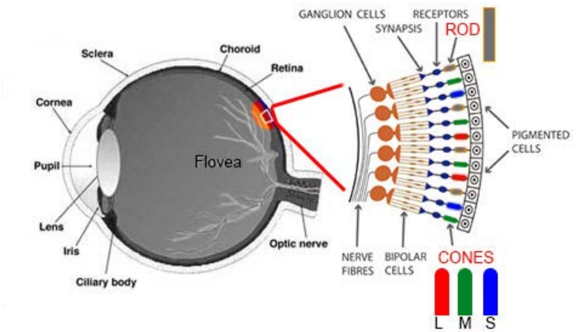

Color mixing

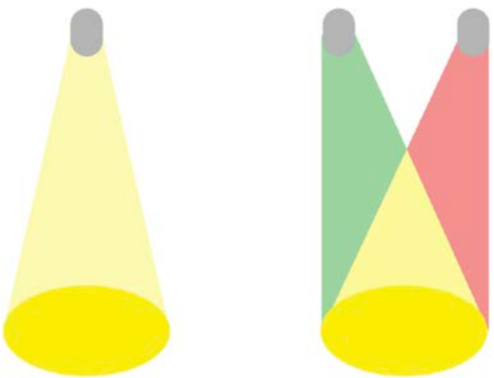

Metamerism effect

Radiative thermal load in visible for a yellow color

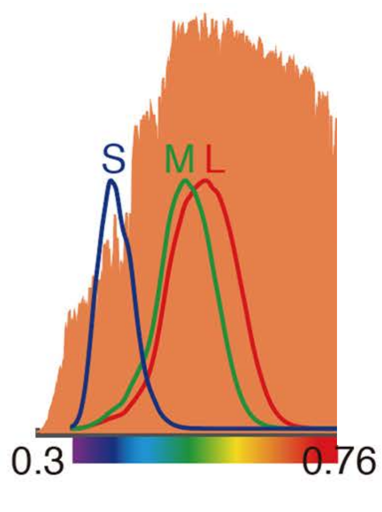

Metamerism effect

376.5 Wm^{-2}

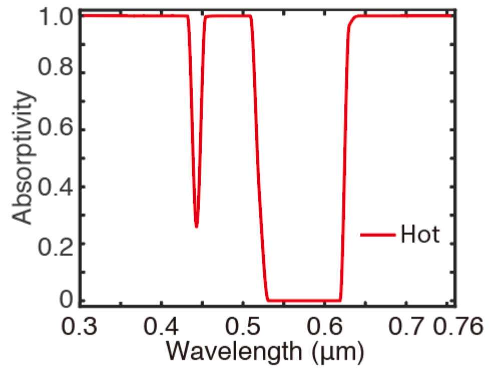

125.5 Wm^{-2}

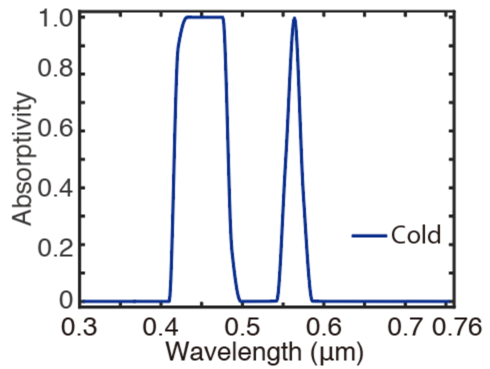

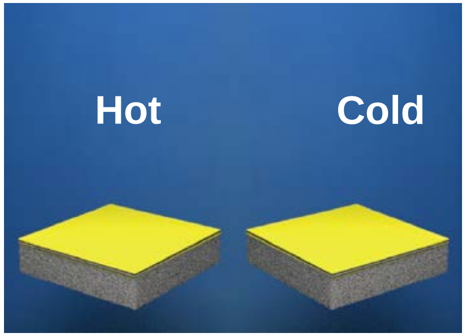

Total radiative thermal load for a yellow color

Hot: 829.7 Wm^{-2}

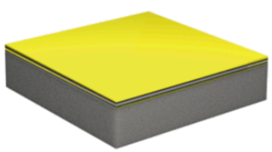

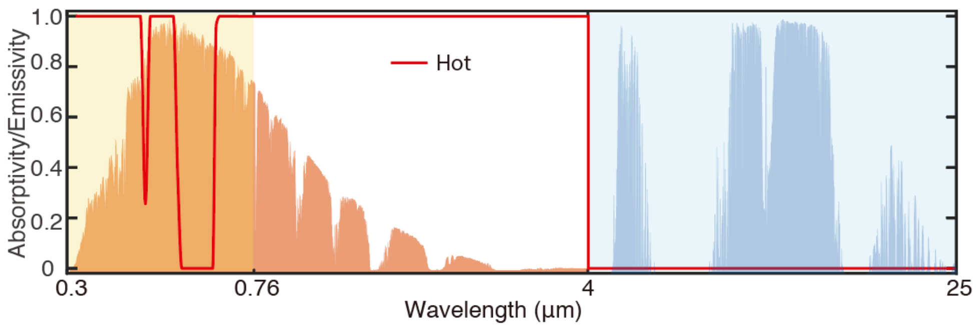

Cold: -4.5 Wm^{-2}

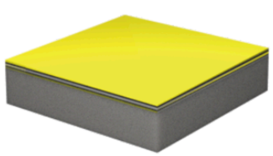

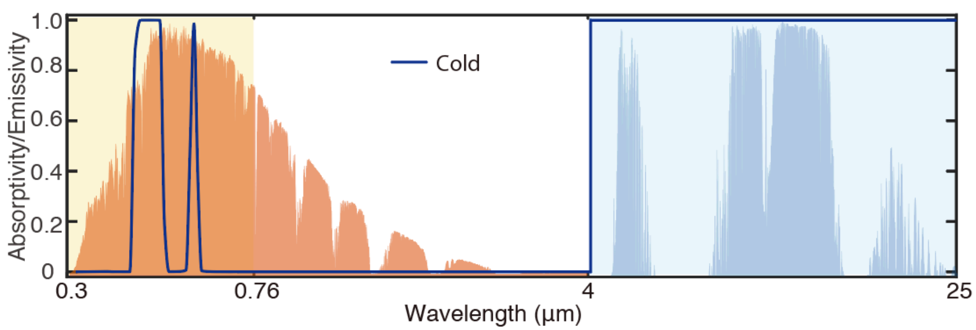

834.2 Wm^{-2}
Tunable range

Range of thermal load of full color space

Lab Color Space

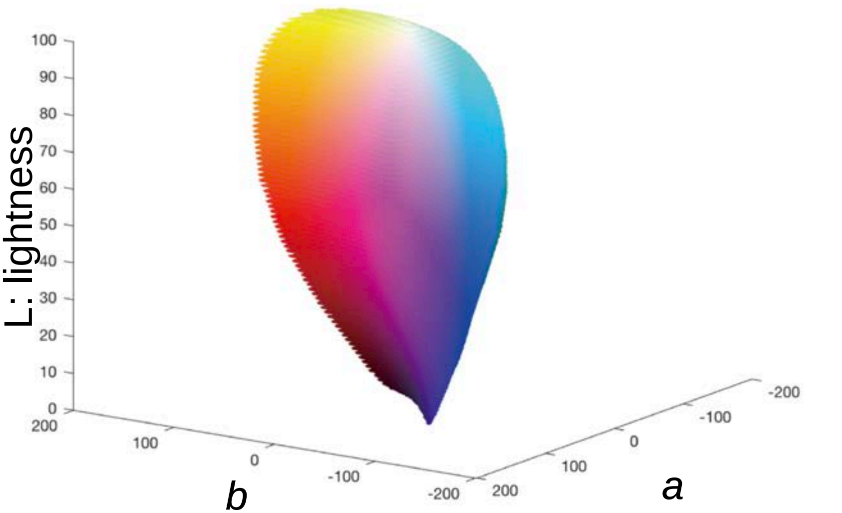

yellowness, blueness.

redness, greenness

Tunable range: 680 to 866 Wm^{-2}

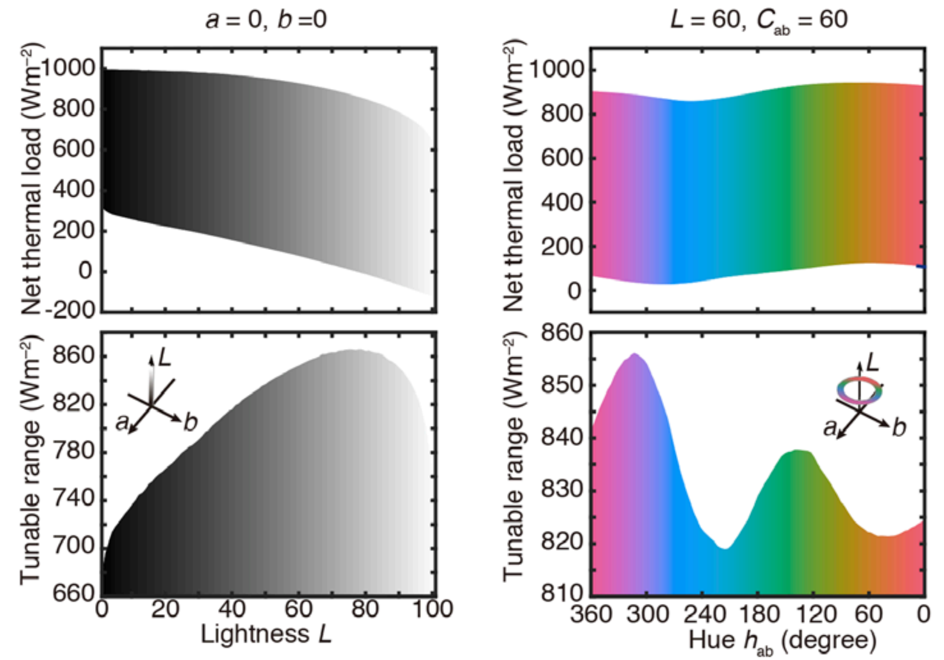

a and *b* determines color chromaticity:
relative saturation, or chroma $C = (a^2 + b^2)^{0.5}$
hue of the colour $h = \arctan(b/a)$,

W. Li, Y. Shi, Z. Chen and S. Fan, Nature Communications 9, 4240 (2018)

Temperature range for colors in an outdoor condition

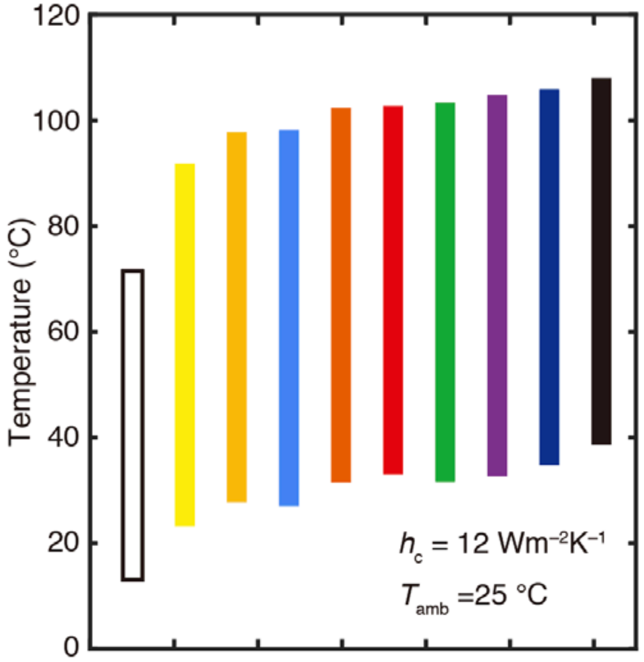

In a typical outdoor condition.

- Same color, temperature can differ by more than 70°C
- A lighter color can be hotter than a darker colour. For example, a light blue color can be over 60°C hotter than a dark blue colour
- A white object can be over 30°C hotter than a black object

W. Li, Y. Shi, Z. Chen and S. Fan, Nature Communications 9, 4240 (2018)

Experiment: two pink object with same color

Hot **Cold**

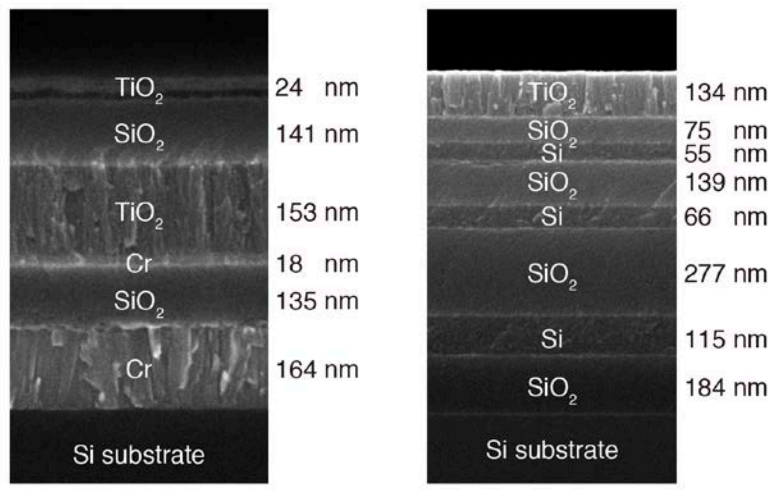

Photonic metamerism effect

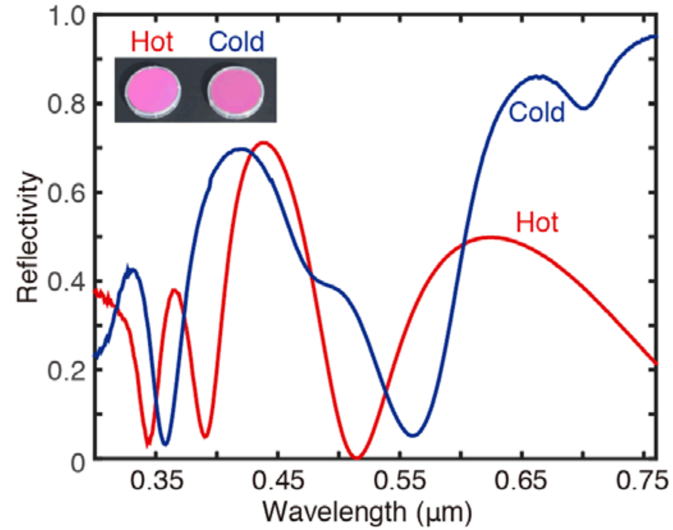

Difference: 100 Wm^{-2}

Experiment: two pink object with same color

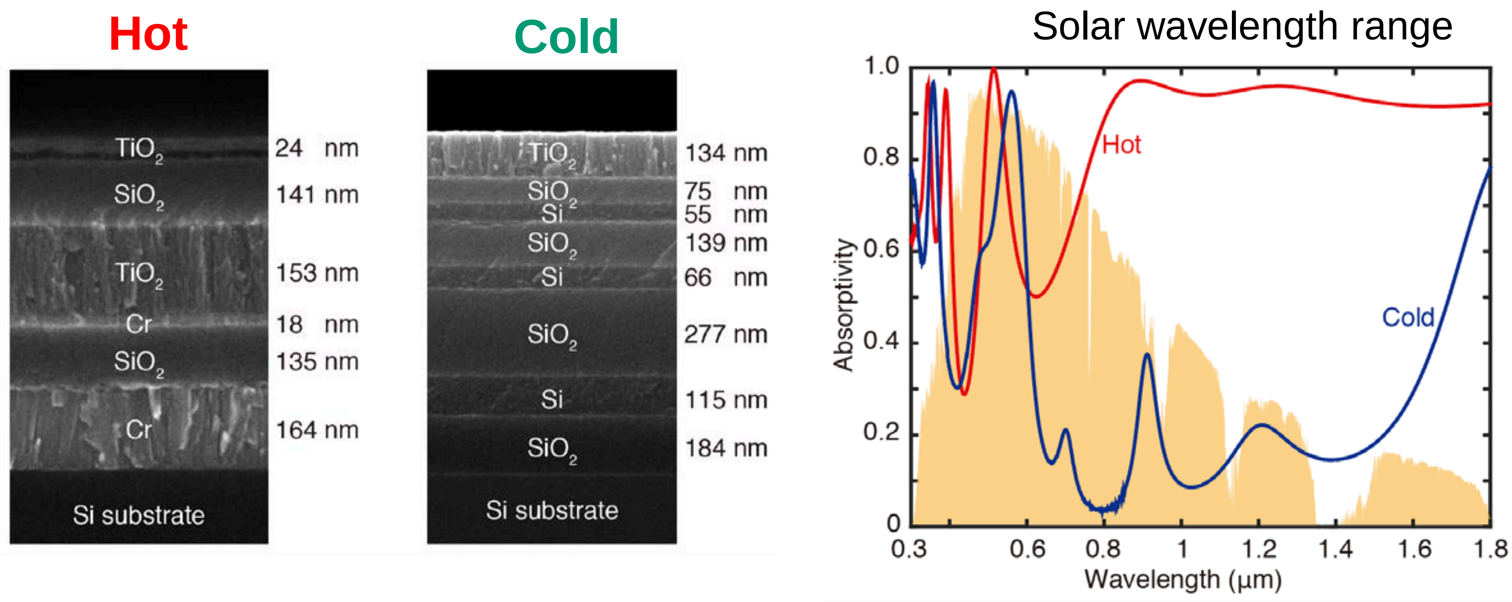

Difference: 400 Wm^{-2}

Experiment: two pink object with same color

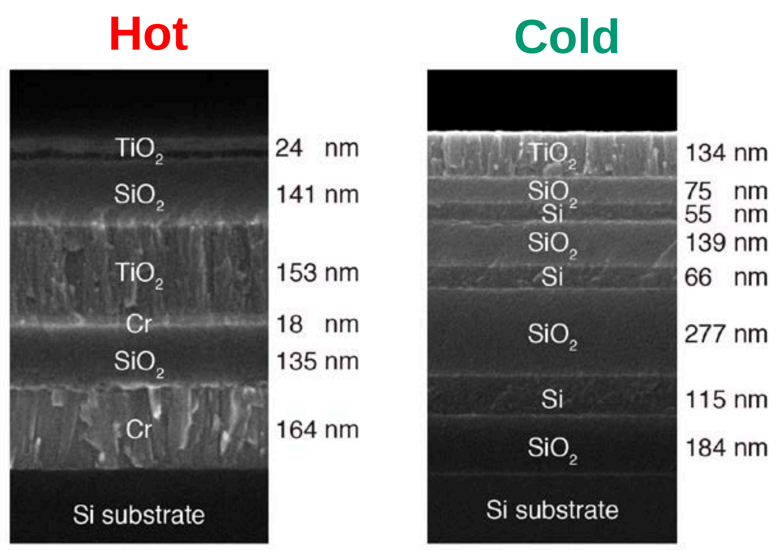

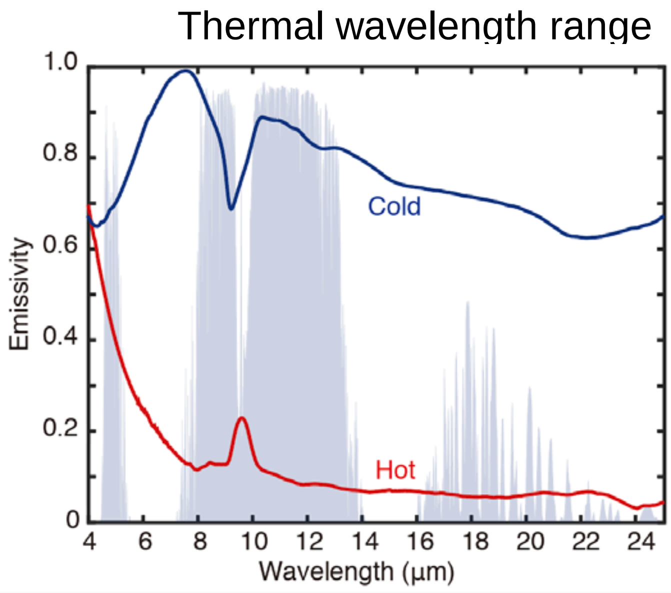

Difference: 86 Wm^{-2}

Experiment: two pink object with same color

Hot Cold

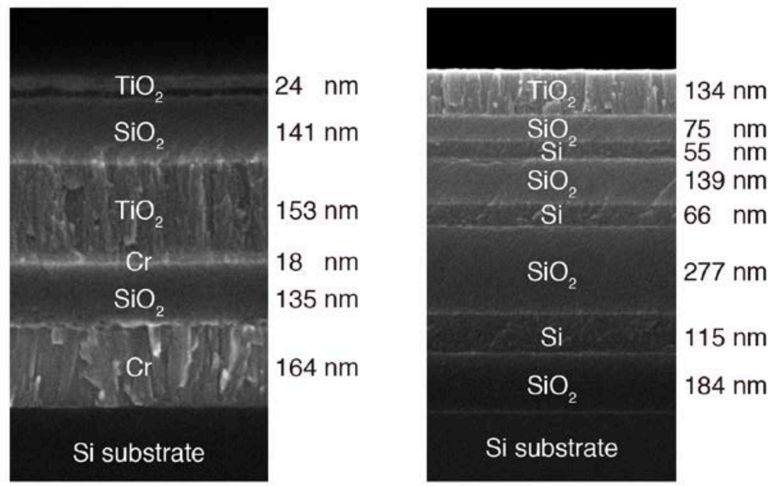

Thermal load:

Hot: 716 Wm^{-2}

Cold: 230 Wm^{-2}

Difference: 486 Wm^{-2}

Outdoor experimental demonstration

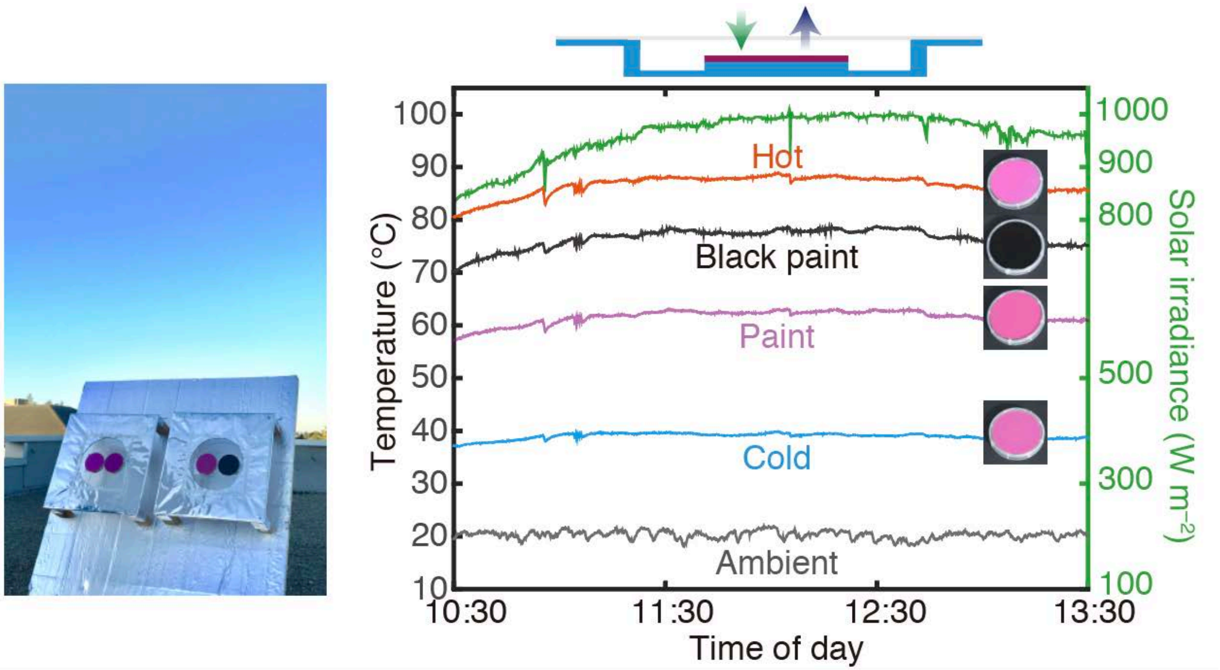

Same color
47.6 °C temperature difference

>20 °C hotter or colder than the pink paint

>10 °C hotter than a black paint

W. Li, Y. Shi, Z. Chen and S. Fan, Nature Communications 9, 4240 (2018)

Outline

Energy technology

Information technology

Fundamental aspects

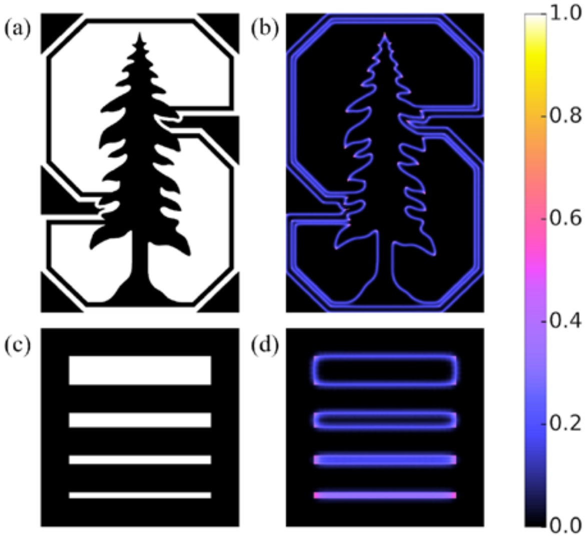

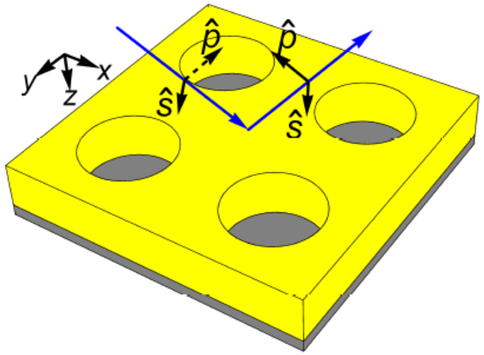

Radiative cooling

Image processing

Topology

Edge detection in human visual system

Edge detection are of fundamental importance in human visual system.

Retinal Neuron

Visual Cortex Neuron

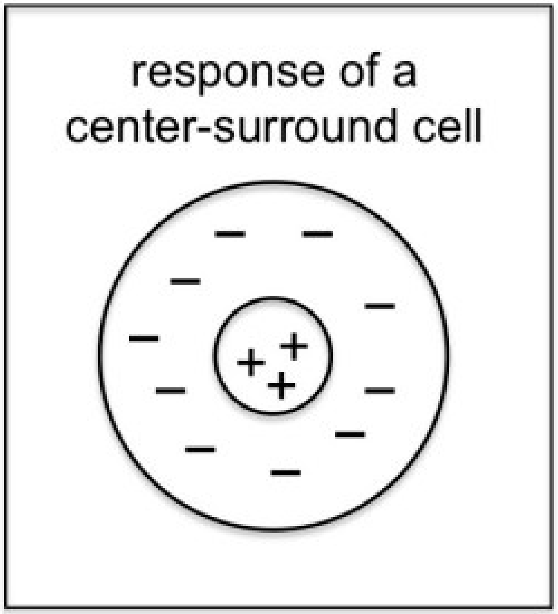

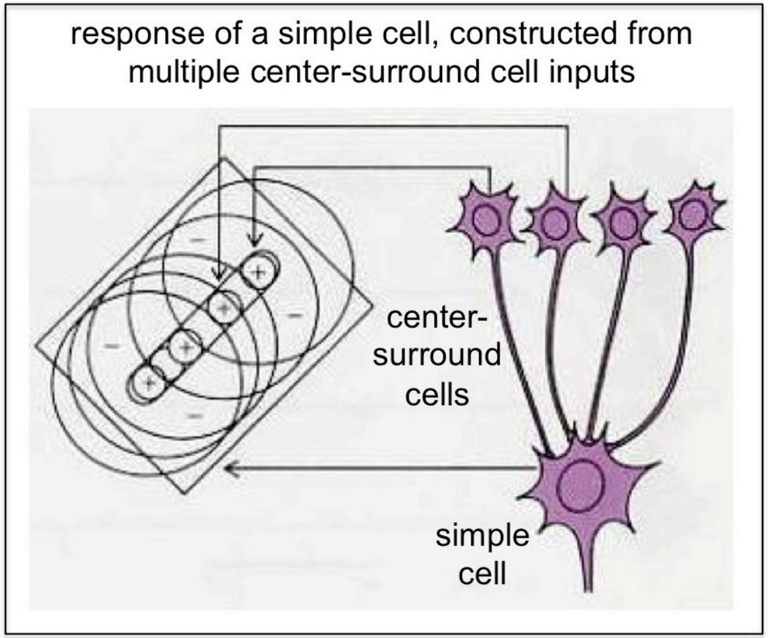

Edge detection is the first layer of human visual perception system.

Hubel D H. Eye, Brain, and Vision. 1981 Nobel Prize with Wiesel.

Edge detection in artificial neural network

Edge detection is a fundamental step in computer vision.

Cat? (0/1)

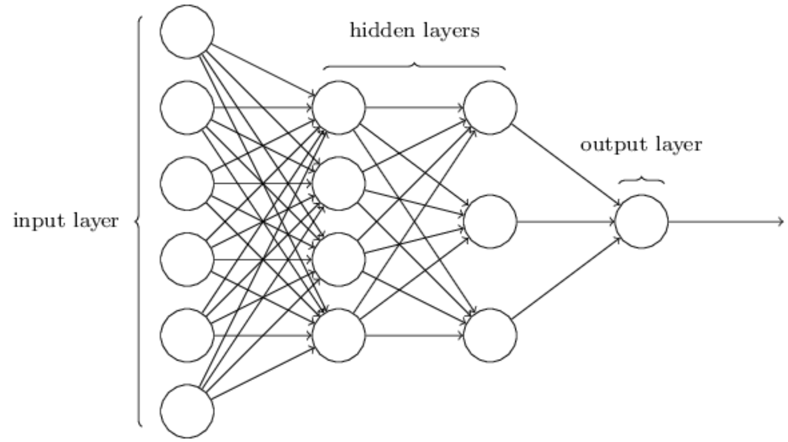

1000×1000

1M 1K 1

Edge detection significantly reduces the amount of data to be processed.
It filters out irrelevant information and preserves important geometric features.

Previous Works

Fourier Optics

Bulk system

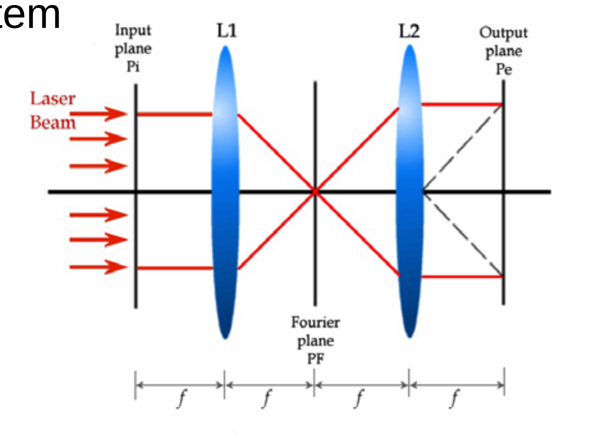

Metasurfaces

1D

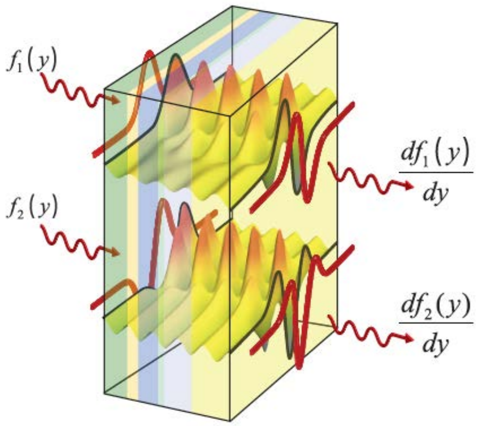

A. Silva et al, Science 343, 160 (2014)
(Engheta and Alu groups)

Spatial differentiation in a standard surface-plasmon geometry

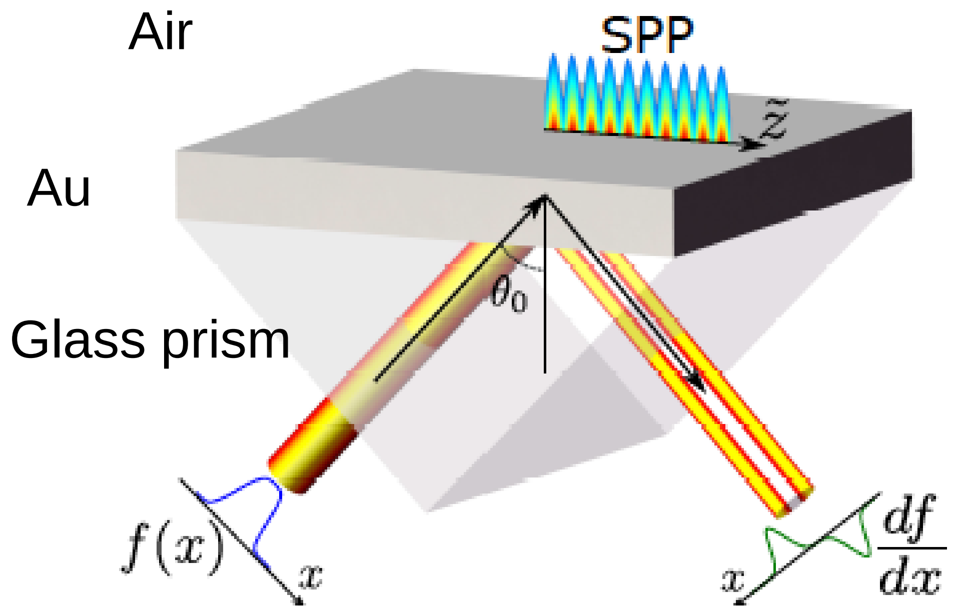

Tengfeng Zhu et al, Nature Communications 8, 15391 (2017).

Collaboration with Professor Zhichao Ruan at Zhejiang University, China

A simple interference picture of the Kretschmann geometry

Direct reflection

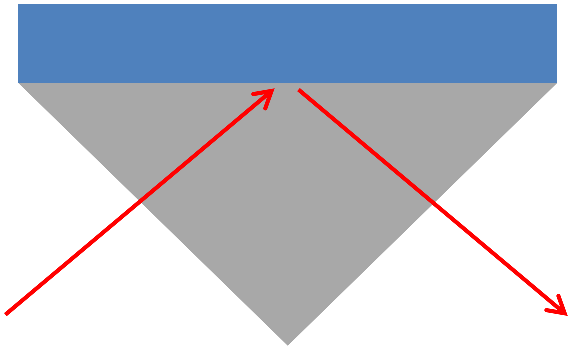

Surface plasmon excitation

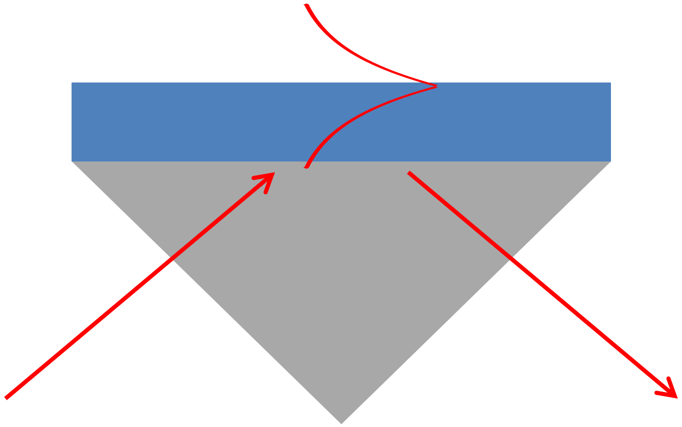

The total reflection coefficient comes from the interference of two pathways

Spatial differentiation at critical coupling

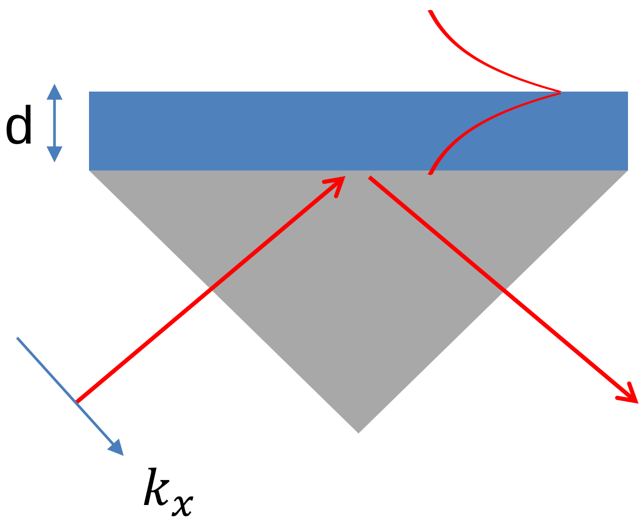

$$H(k_x) = e^{i\phi} \frac{ik_x + \dfrac{\alpha_{spp} - \alpha_l}{cos\theta_0}}{ik_x + \dfrac{\alpha_{spp} + \alpha_l}{cos\theta_0}}$$

When $\alpha_{spp} = \alpha_l$

$$H(k_x) = C \cdot k_x$$

At critical coupling, we have spatial differentiation

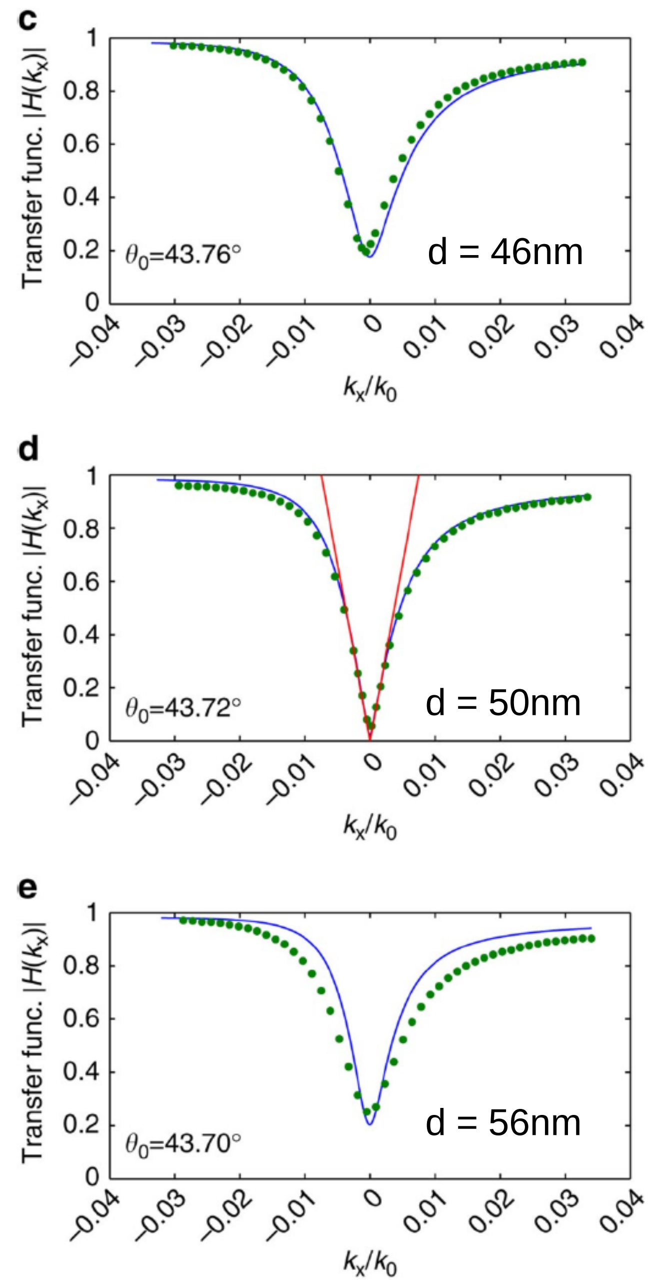

Experimental setup

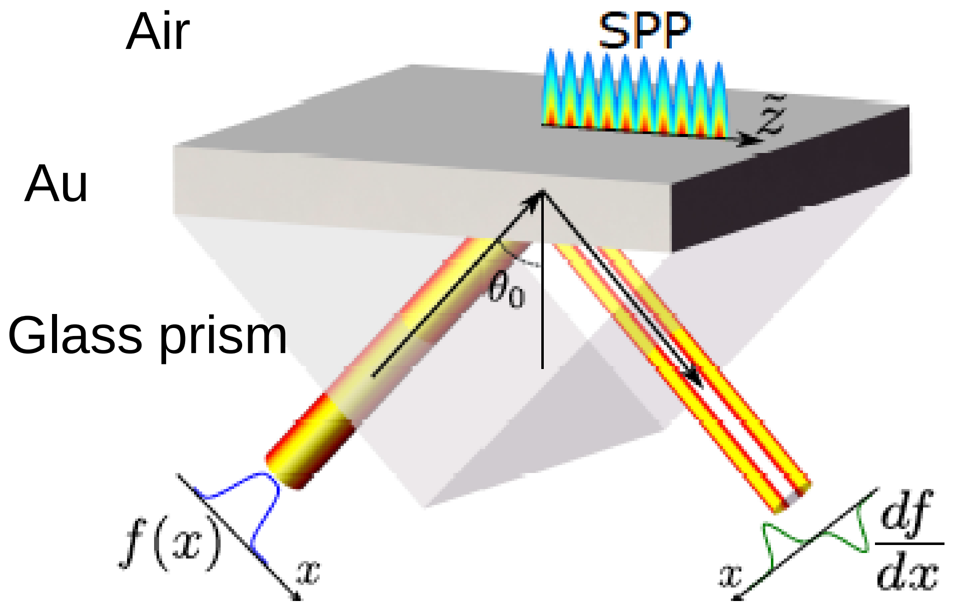

Spatial light modulator to generate input beam profile

Image reflected field pattern

Edge detection

Input **Output**

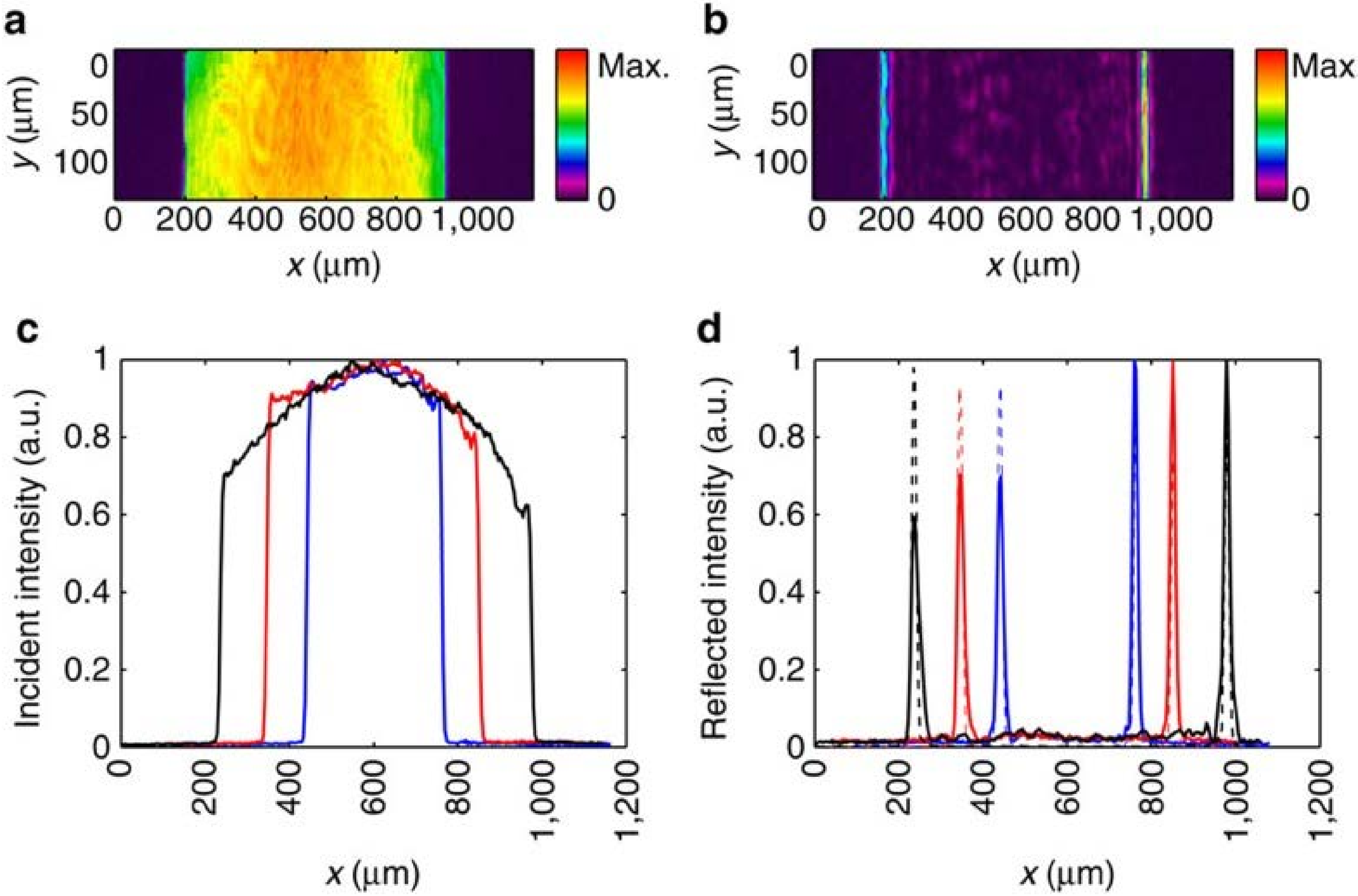

Spatial resolution of neighboring edges

Input

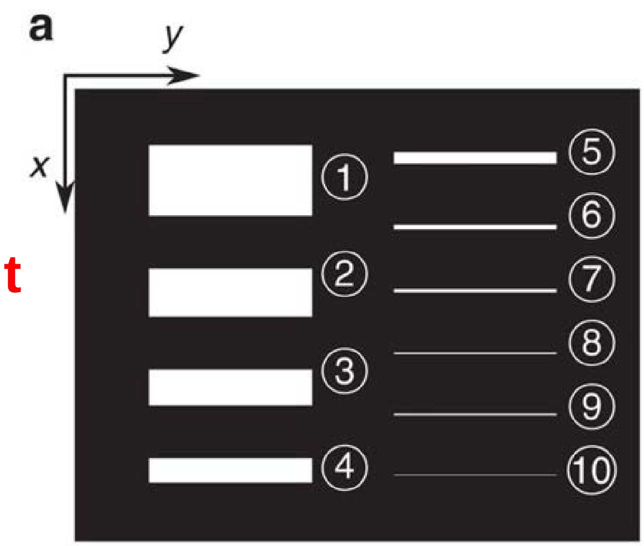

Output Experiment

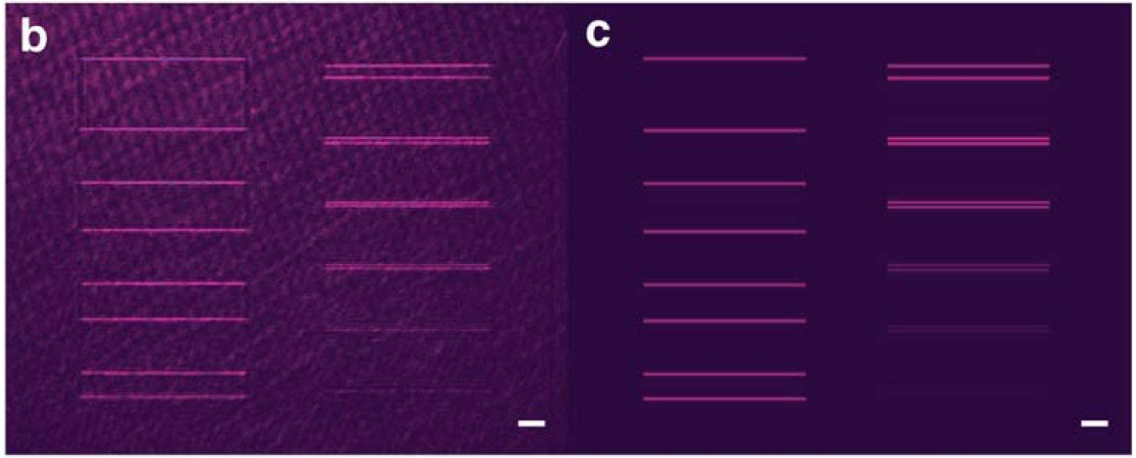

Output Simulation

①	②	③	④	⑤	⑥	⑦	⑧	⑨	⑩
273.6	184.8	139.2	93.6	45.6	19.2	12.0	7.2	4.8	2.4

Resolution: 7.5 micron

Detecting edges in both amplitude and phase distribution

Amplitude modulation

Phase modulation

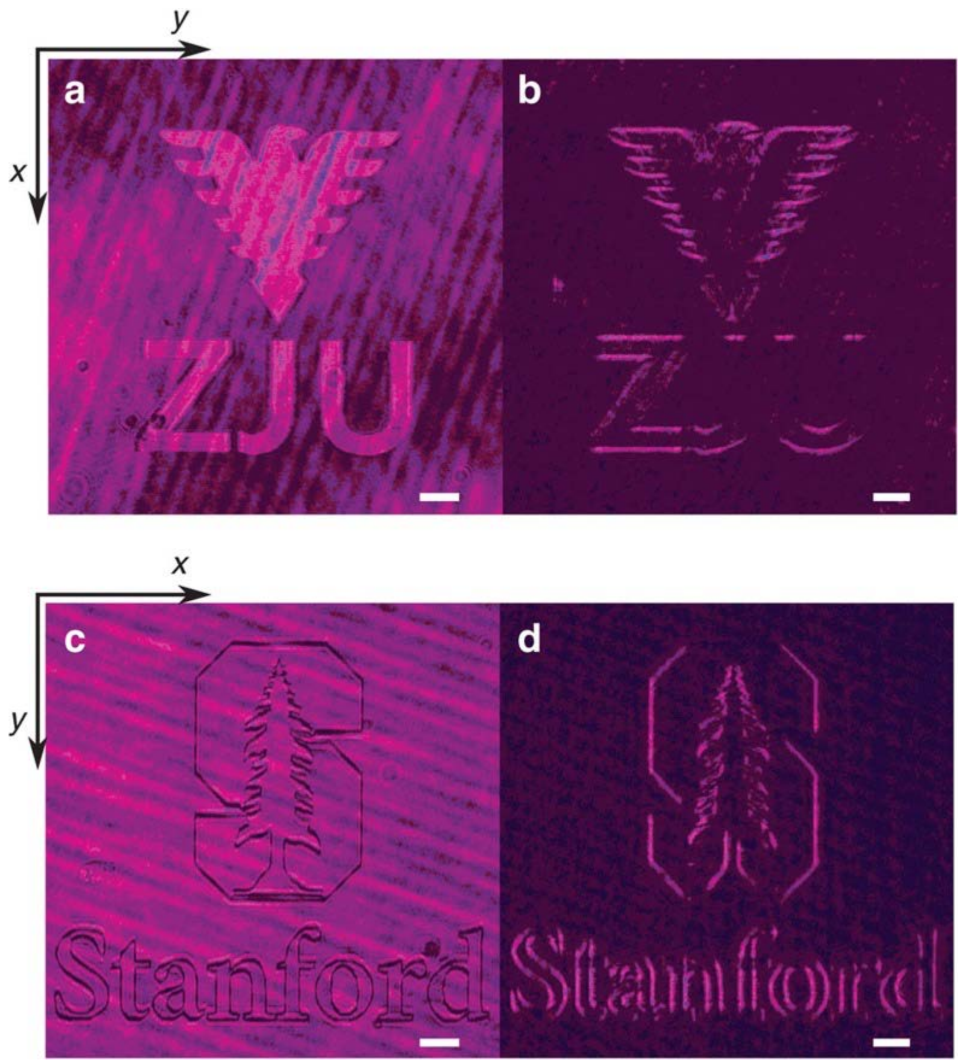

Input **Output**

Going from 1D to 2D

$f(x,y)$ Thin film $\nabla^2 f(x,y)$

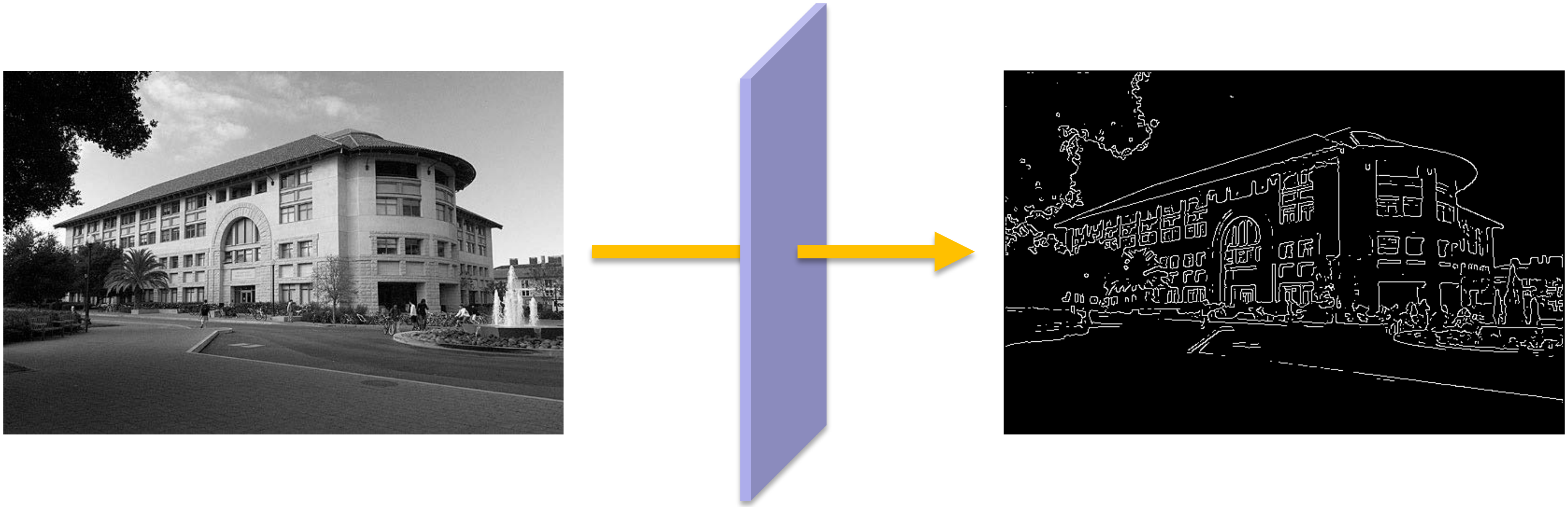

Normal incidence, Transmission mode
2D differentiation

Laplacian as an isotropic 2D derivative operator

- The Laplacian is the lowest order linear combination of partial derivatives that is isotropic.
- Widely used for edge detection purposes.

Real space

$$g(x,y) \propto \nabla^2 f(x,y) = (\partial_x^2 + \partial_y^2) f(x,y)$$

Wavevector space

$$\tilde{g}(k_x,k_y) = t(k_x,k_y)\,\tilde{f}\,(k_x,k_y) \propto (k_x^2 + k_y^2)\tilde{f}\,(k_x,k_y)$$

$$t(\boldsymbol{k} = \boldsymbol{0}) = 0$$

Guided resonances in e.g. a photonic crystal slab

Bright state at normal incidence are two-fold degenerate

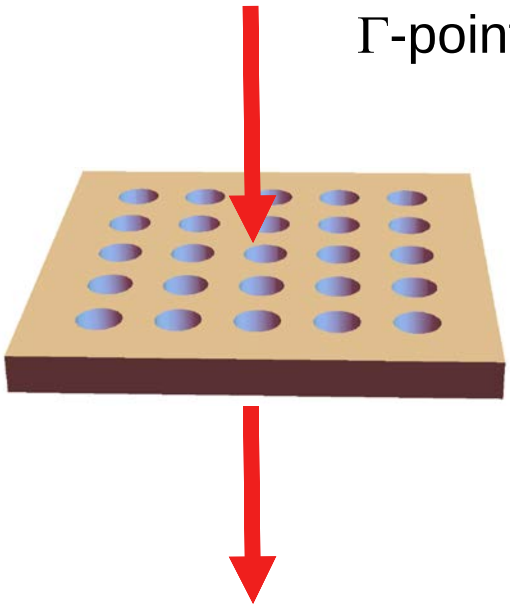

For normally incident light

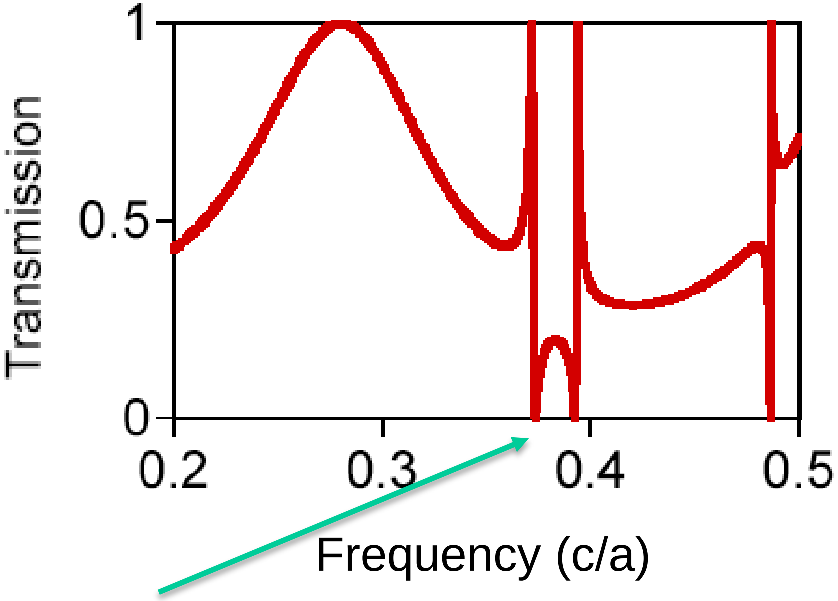

Guided resonance

S. Fan and J. D. Joannopoulos, Physical Review B 65, 235112 (2002).

Theoretical Criteria

Requires an isotropic band structure

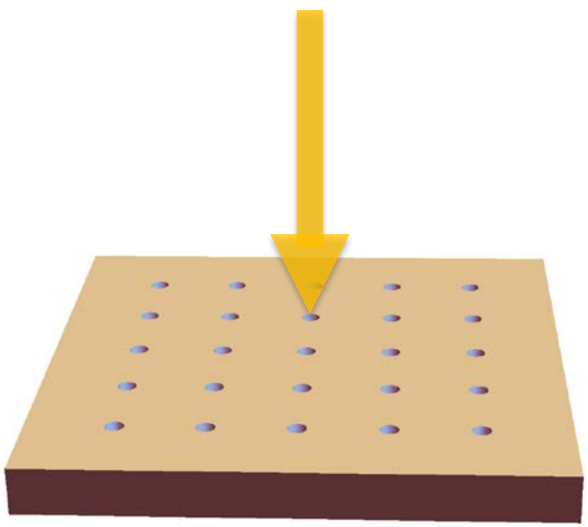

$$t(k) \propto \delta\omega_0(k) \propto k^2$$

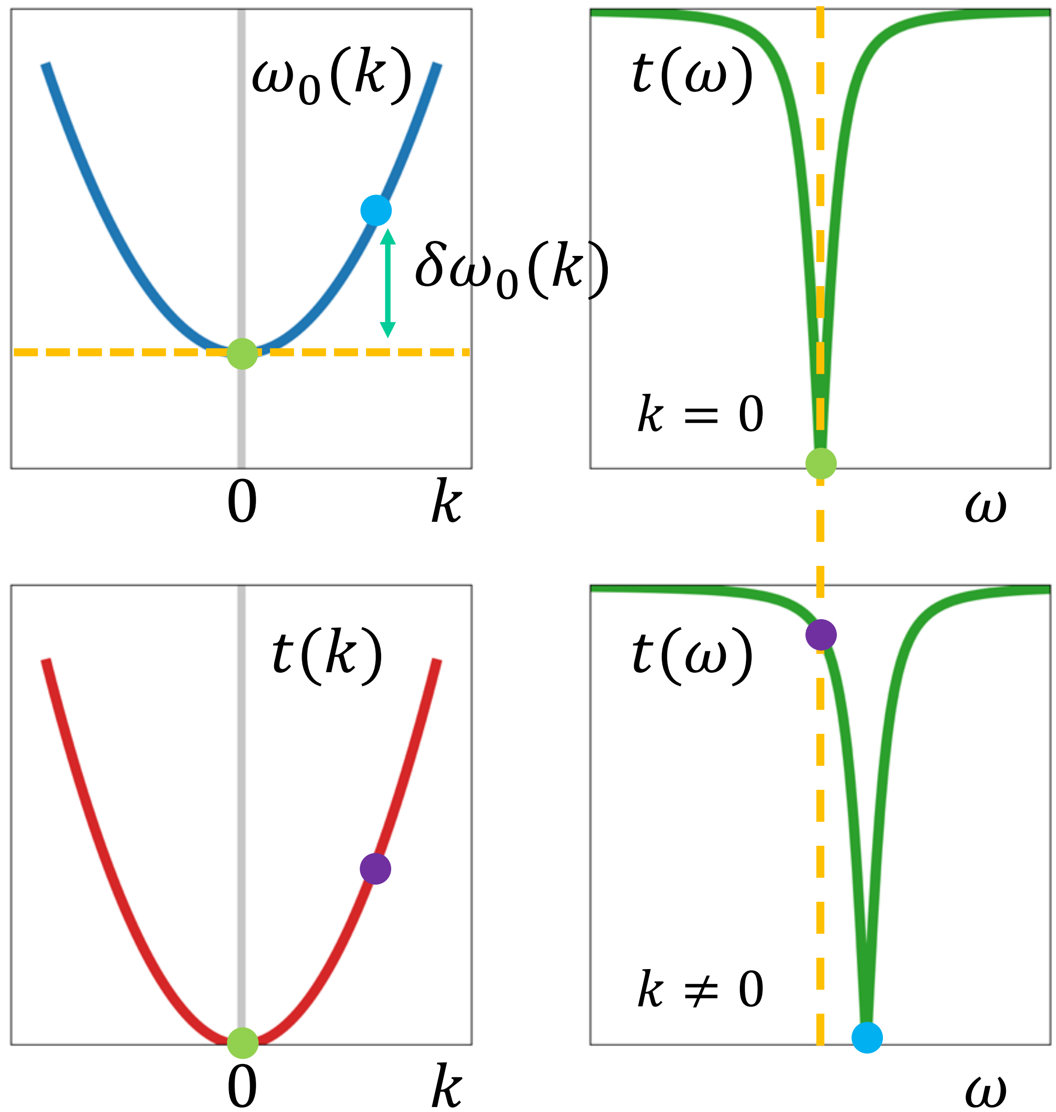

Bright state at normal incidence are two-fold degenerate

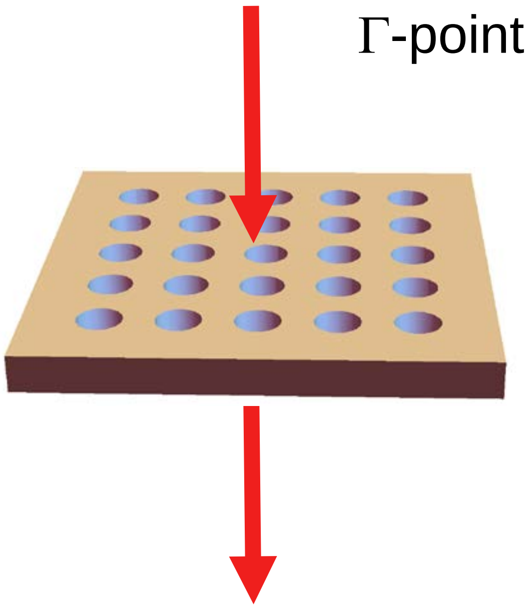

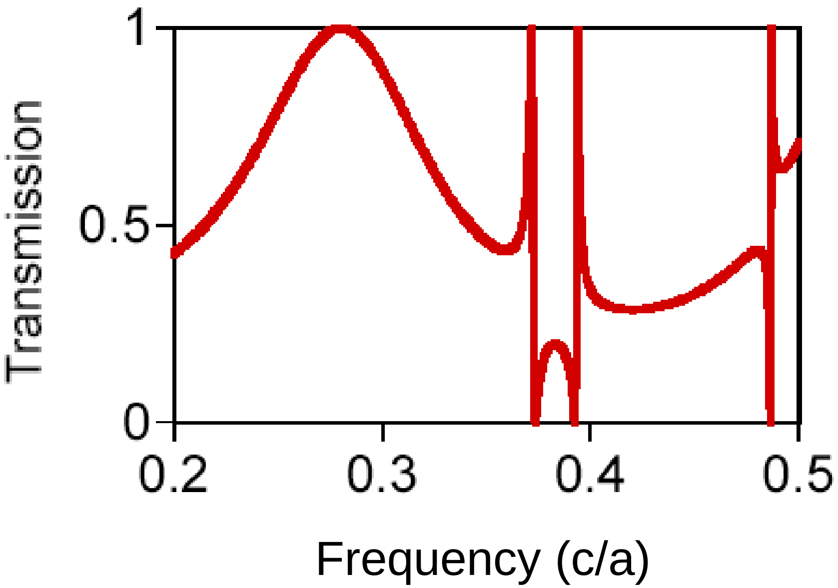

The plane wave at normal incidence belongs to a two-dimensional irreducible representation,

Hence the guided resonance at normal that can couple to plane wave also must belong to a two-dimensional irreducible representation

S. Fan and J. D. Joannopoulos, Physical Review B 65, 235112 (2002).

k . p analysis of bandstructure around Γ point

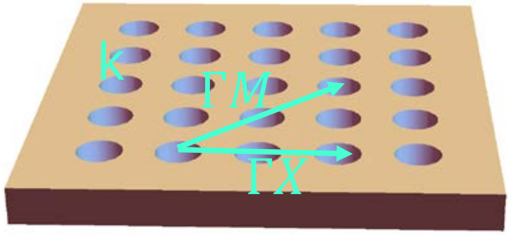

$$H(k) = (\omega_0 + a|k|^2)I + b\left(k_x^2 - k_y^2\right)\sigma_z + c k_x k_y \sigma_x$$

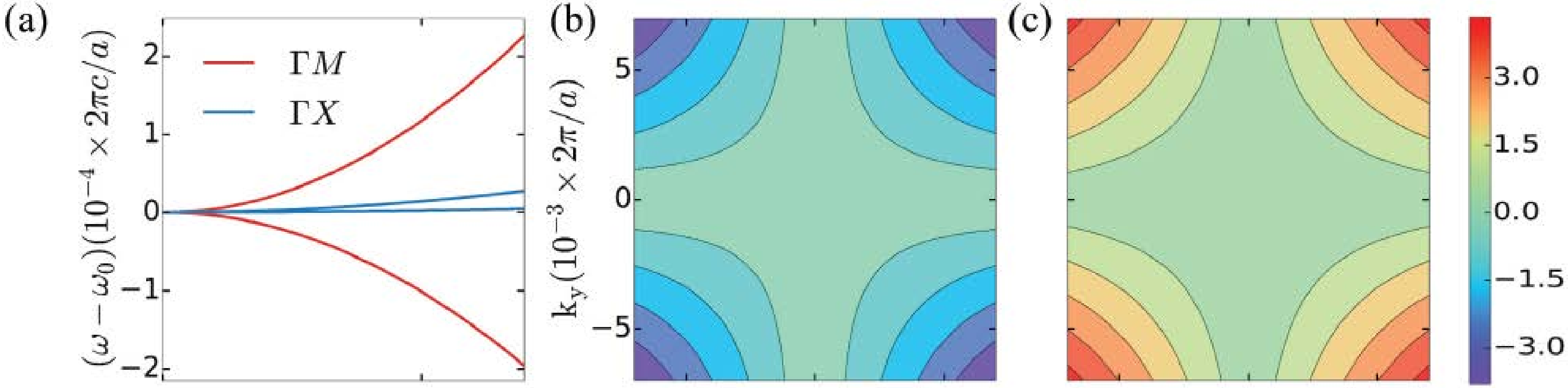

The band structure around the Γ point is typically highly anisotropic.
One can not use typical photonic crystal slab structure to achieve Laplacian

Isotropic Band Structure

$r = 0.11a$

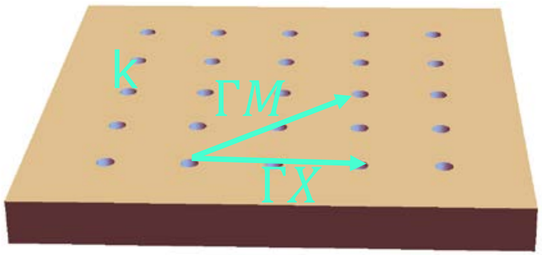

$d = 0.55a$

$$H(k) = (\omega_0 + a|k|^2)I + b\left(k_x^2 - k_y^2\right)\sigma_z + ck_xk_y\sigma_x$$

with

$b = 0, and\ c = 0$

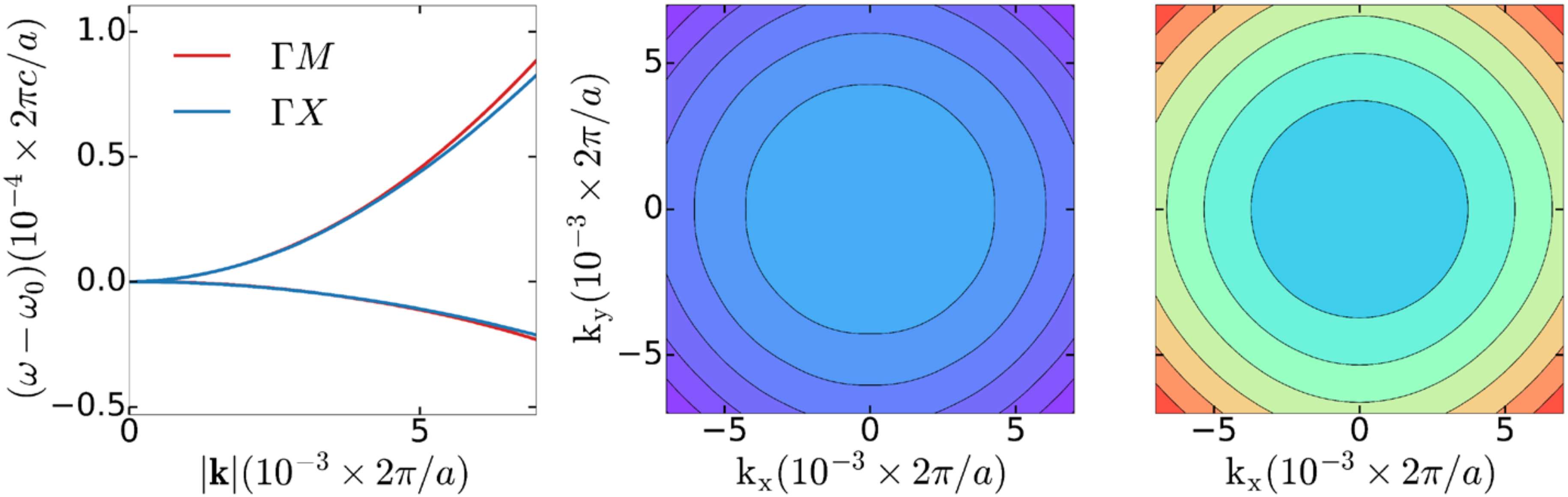

Isotropic Transmission

$(|t_{sp}| = |t_{ps}| = 0)$

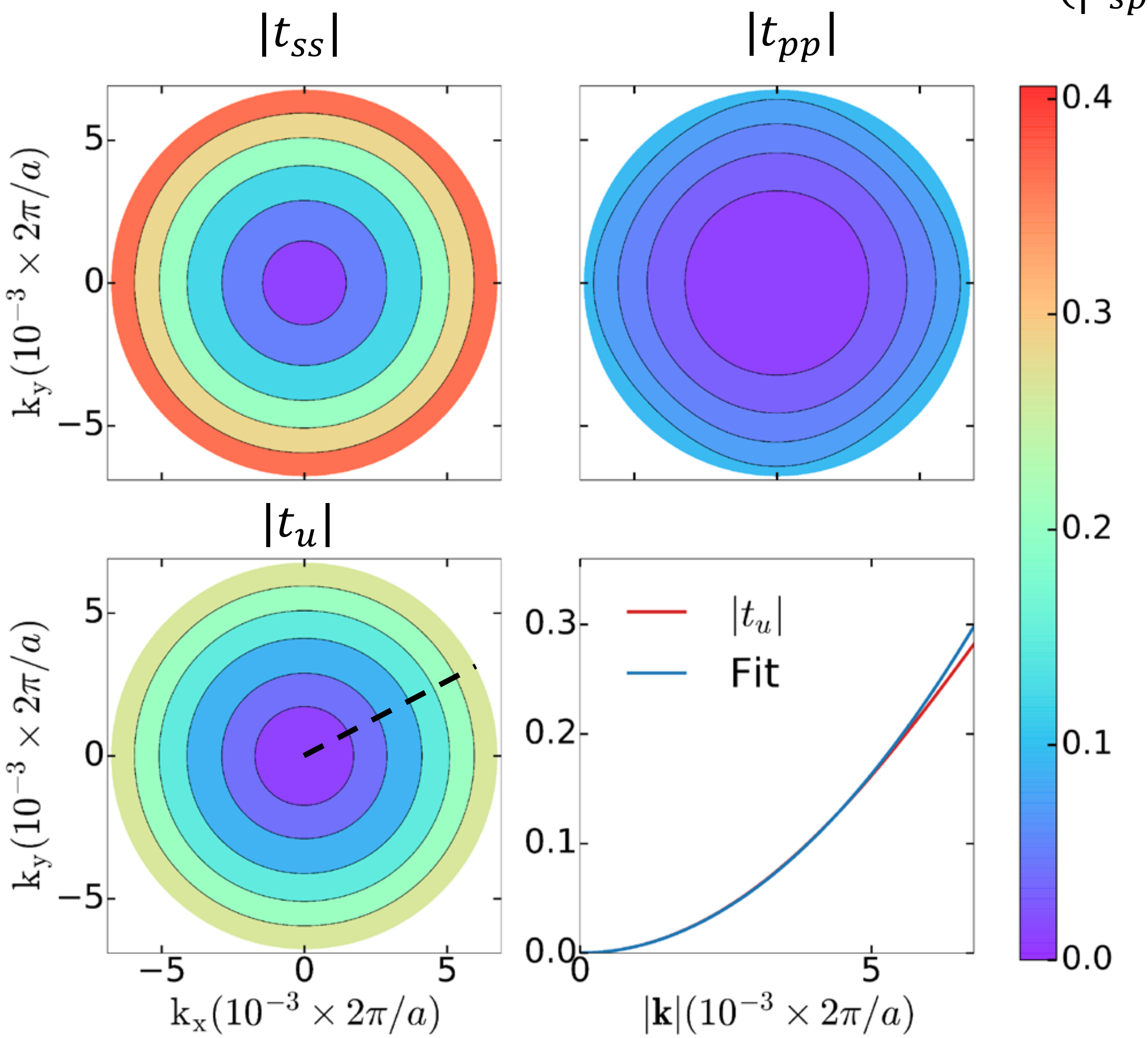

Numerical Demonstration

2610 a*1728 a

500 a*
(100, 50, 30, 20) a

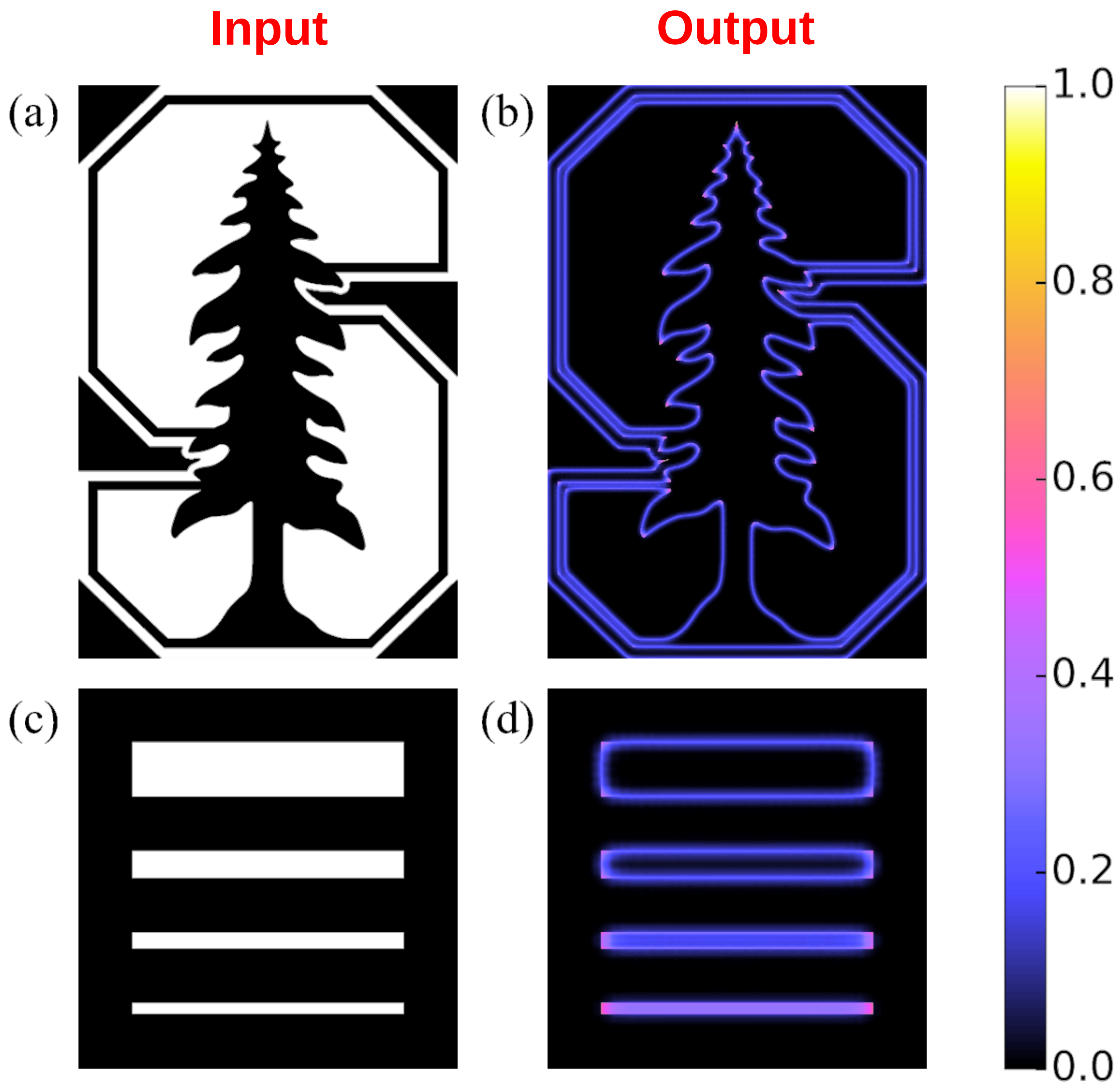

Design for visible image processing with different optical functionalities for reflection/transmission and on/off resonance

Transmission

Si_3N_4
Visible

Reflection

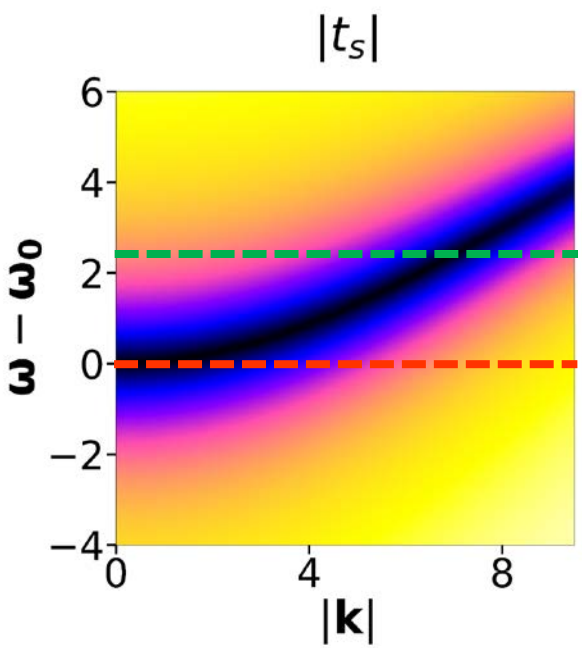

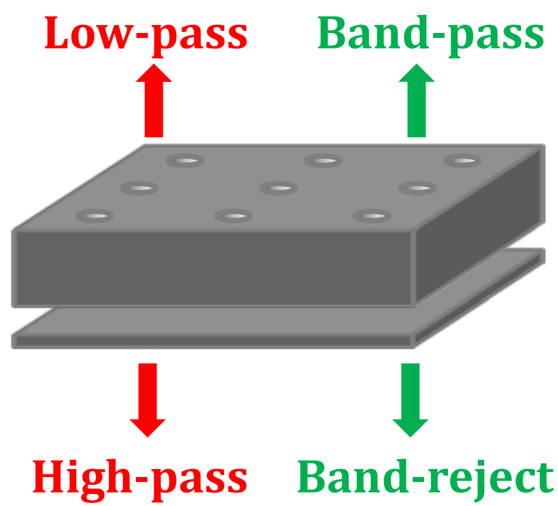

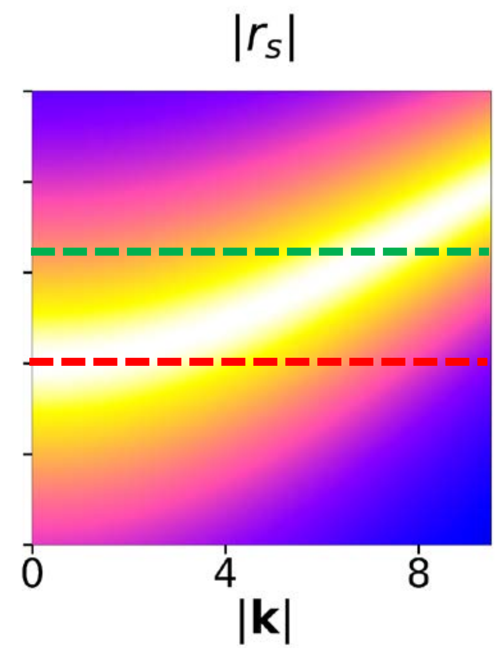

C. Guo, M. Xiao, M. Minkov, Y. Shi, and S. Fan, Journal of the Optical Society of America A 35, 1685 (2018).

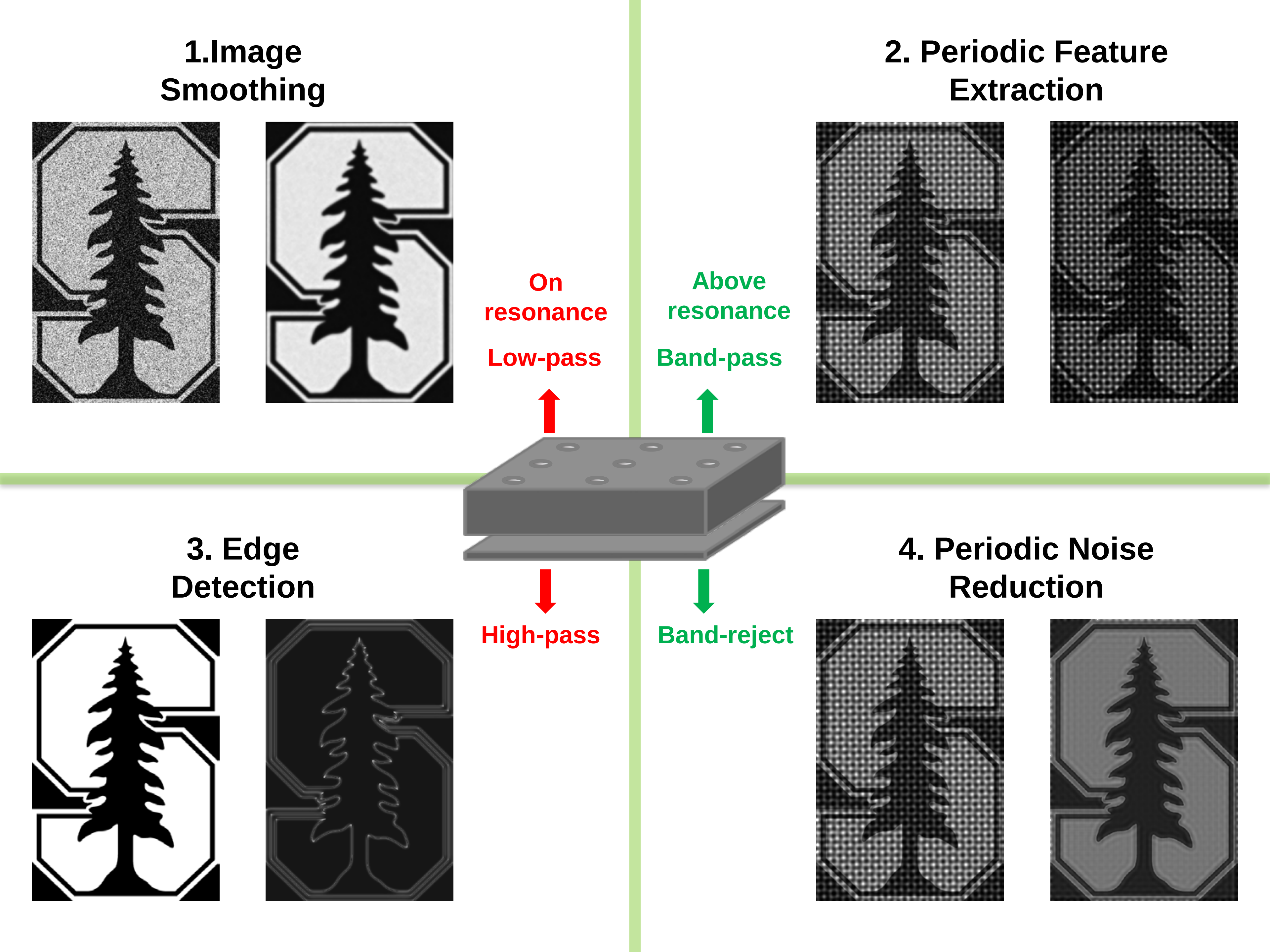

1.Image Smoothing
2. Periodic Feature Extraction
On resonance
Low-pass
Above resonance
Band-pass
3. Edge Detection
4. Periodic Noise Reduction
High-pass
Band-reject

Outline

Energy technology

Information technology

Fundamental aspects

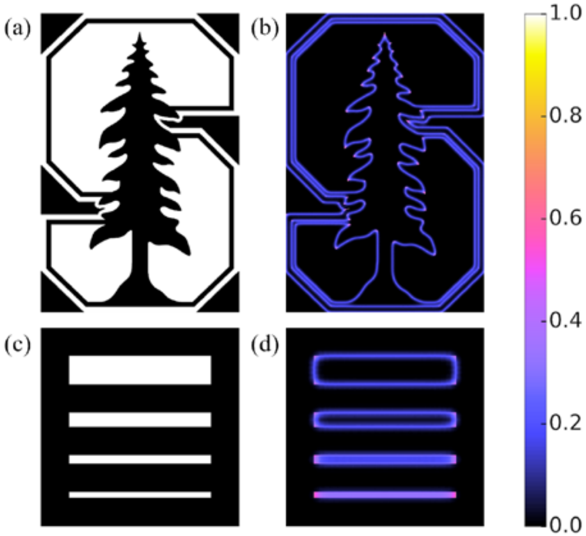

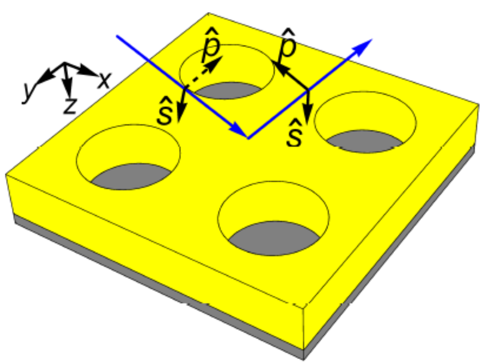

Radiative cooling

Image processing

Topology

A bit of mathematical background: Index of a vector field

A real two-dimensional vector field on a two-dimensional surface supports topological singularity, where the vector field vanishes.

The fashion at which the field winds around the singularity defines the index, or the topological charge of the singularity

Index = +1

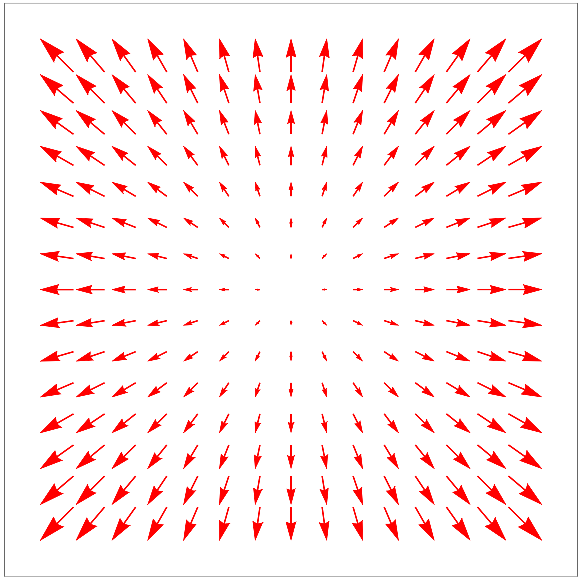

Index = -1

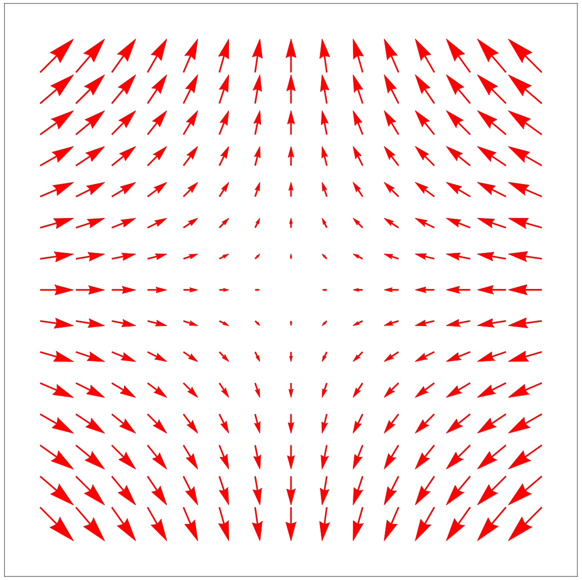

Polarization Conversion

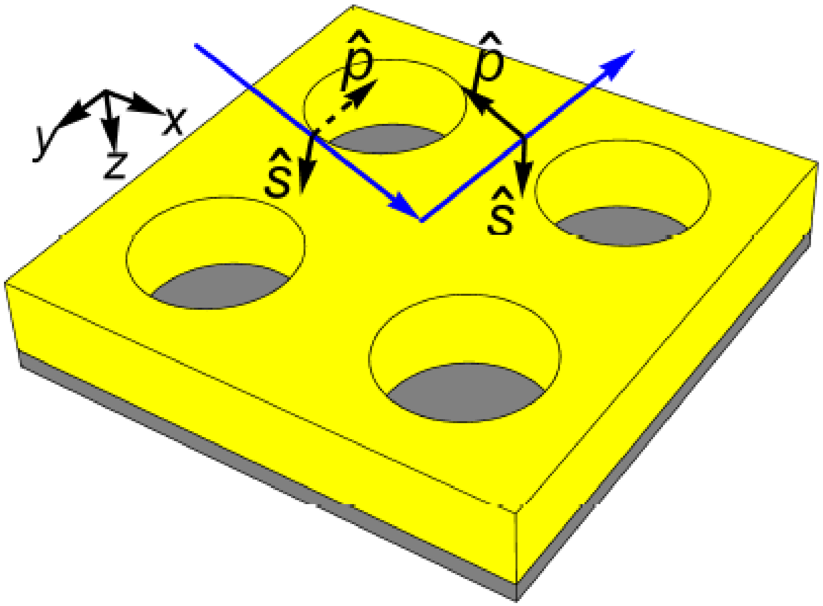

- Sub-wavelength periodicity. No diffraction.
- Assuming a back-mirror, completely intensity reflection.
- The system completely characterized by the reflection matrix:

$$R = \begin{bmatrix} R_{SS} & R_{SP} \\ R_{PS} & R_{PP} \end{bmatrix}$$

$R_{SS} = 0$ implies complete polarization conversion

$R_{SS}(k_x, k_y)$ represents a complex field in a two-dimensional plane, hence it can support topological singularity.

The effect of complete polarization conversion thus can have topological features.

Complete Polarization Conversion

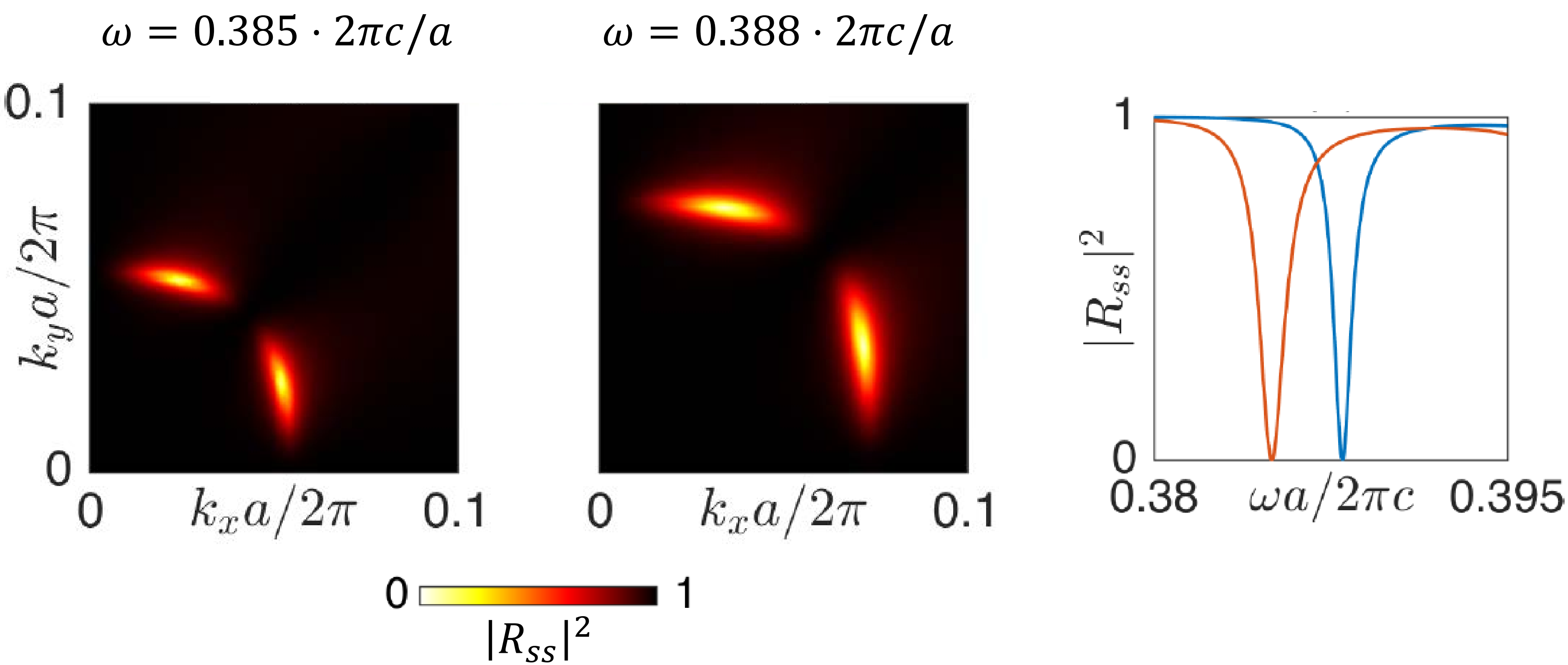

Robust over frequency variation:

Over a wide range of frequencies, $0.35c/a$ to $0.4c/a$, at each frequency, there is always a wavevector where complete polarization conversion occurs

Y. Guo, M. Xiao, and S. Fan, Physical Review Letters 119, 167401 (2017).

Topological charge in the reflection coefficient

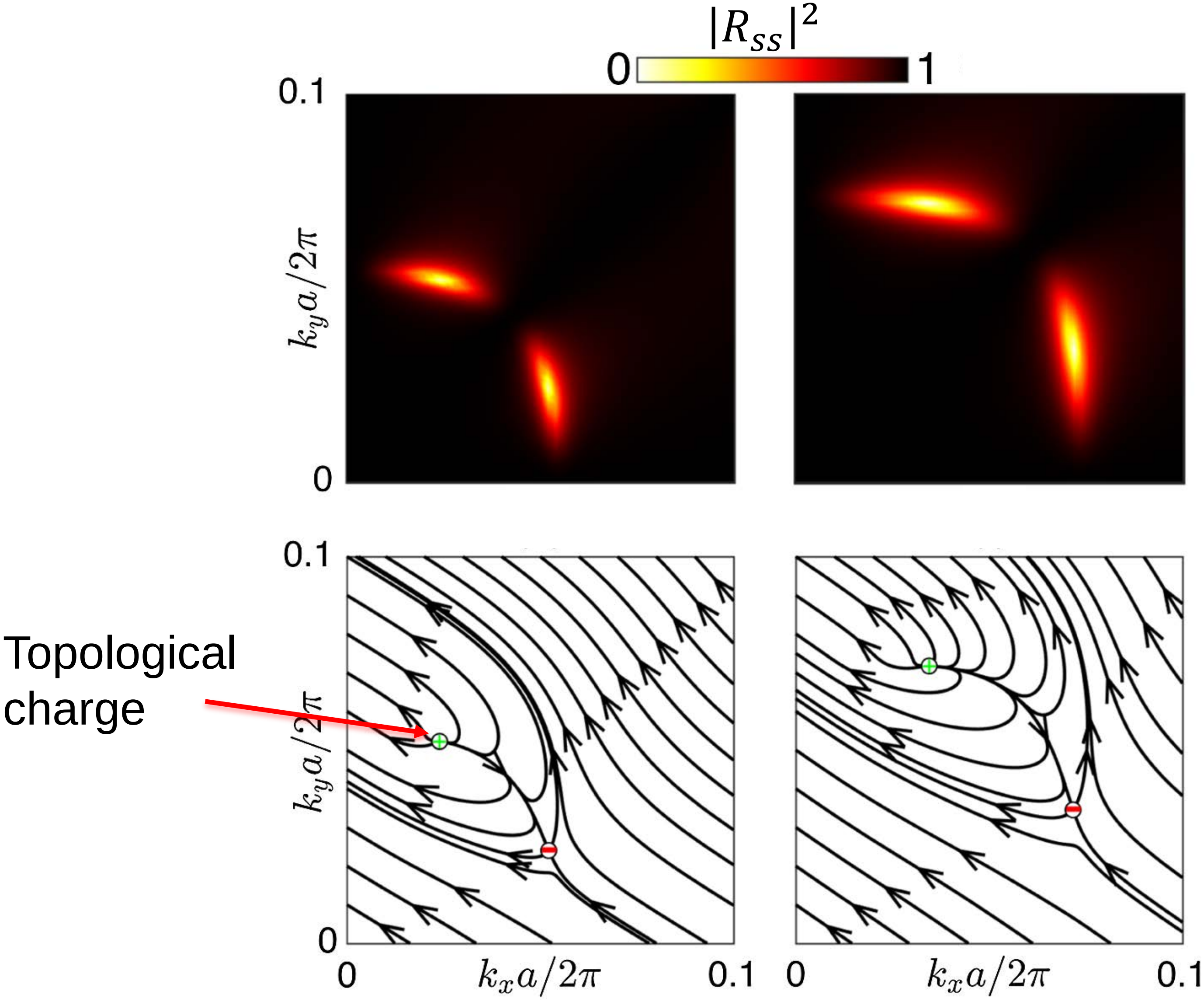

Vector plot of the complex R_{ss}

$(Re(R_{ss}), Im(R_{ss}))$

Non-zero winding number around the point where $R_{ss} = 0$

Y. Guo, M. Xiao, and S. Fan, Physical Review Letters 119, 167401 (2017).

Polarization conversion from guided resonance

Guided resonance can couple to both s and p polarizations

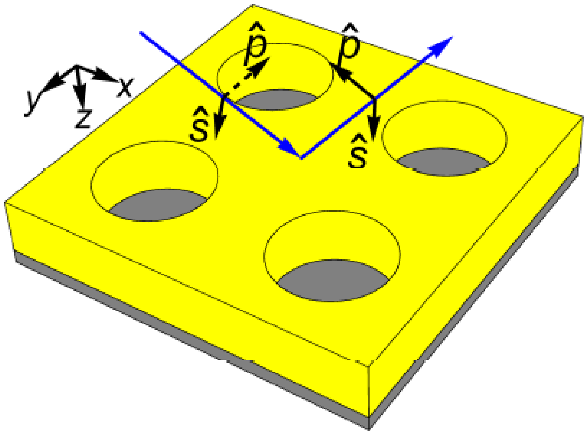

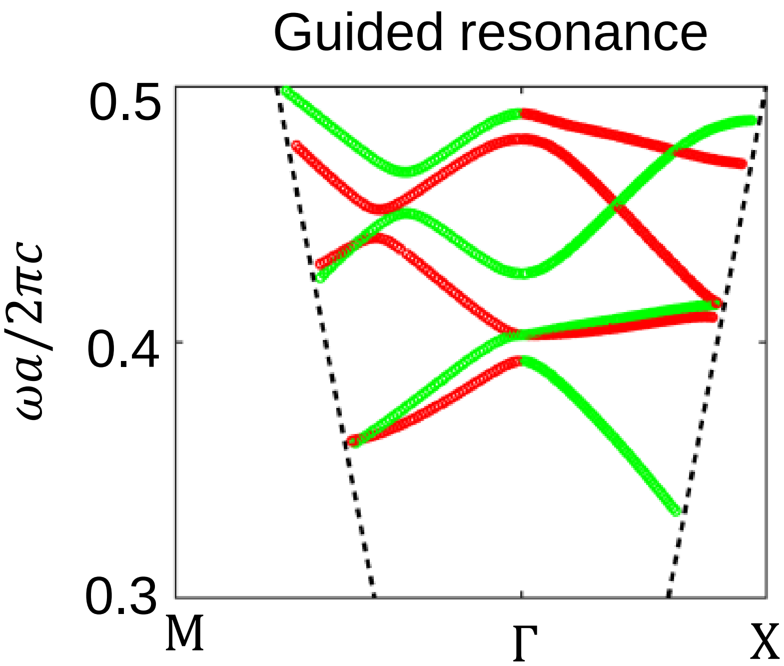

$$R_{ss} \propto 1 - \frac{|d_s|^2}{i(\omega_0 - \omega) + (|d_s|^2 + |d_p|^2)/2}$$

Complete polarization conversion occurs when $|d_s| = |d_p|$

Y. Guo, M. Xiao, and S. Fan, Physical Review Letters 119, 167401 (2017).

Geometric proof of complete polarization conversion

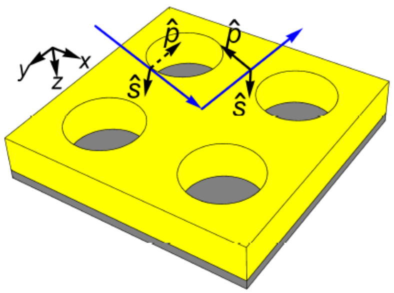

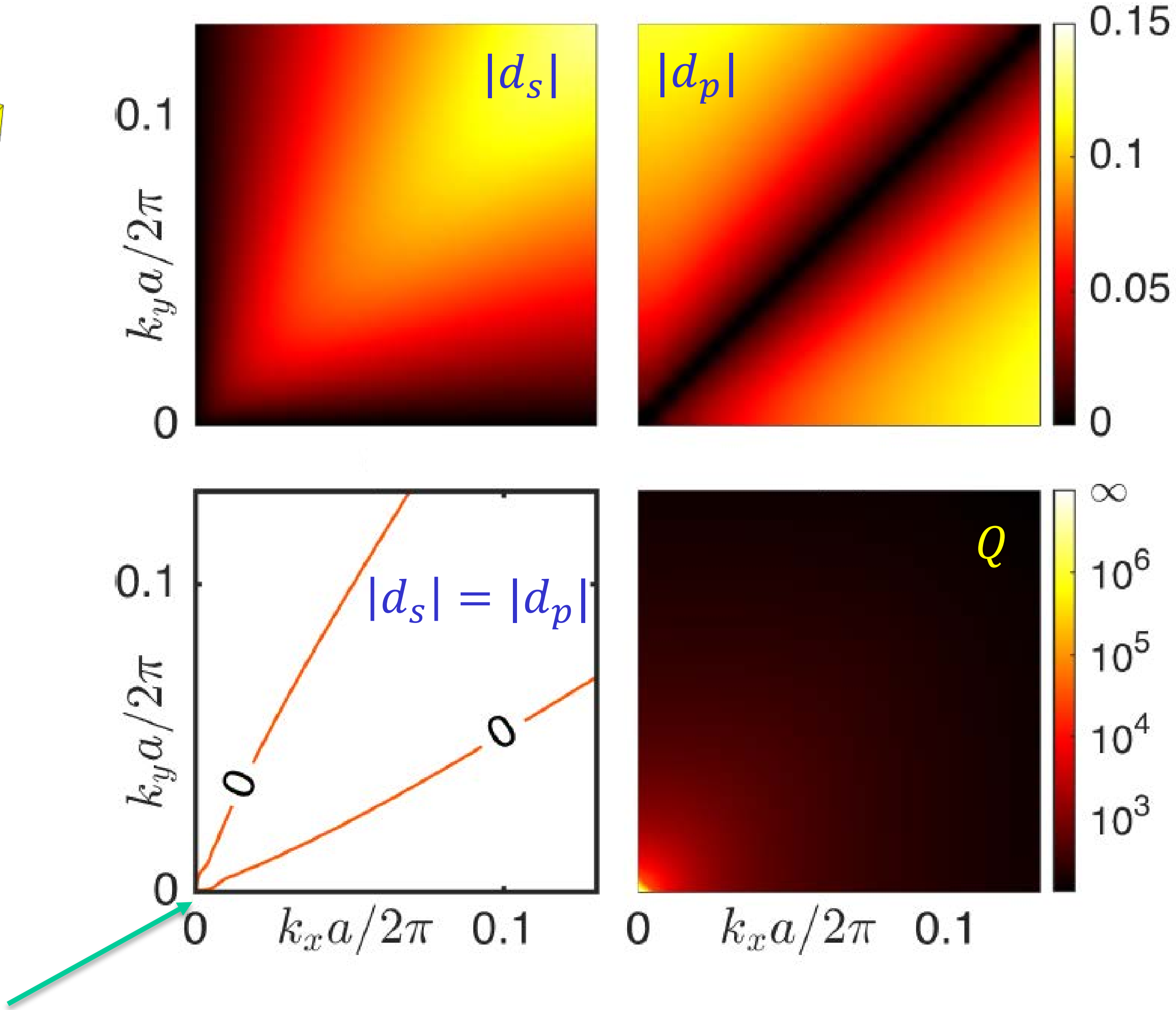

Mirror planes

$$k_x = 0$$
$$k_y = 0$$
$$k_x = k_y$$

Symmetry Protected Bound State In Continuum

Arbitrary polarization conversion in a single meta-surface

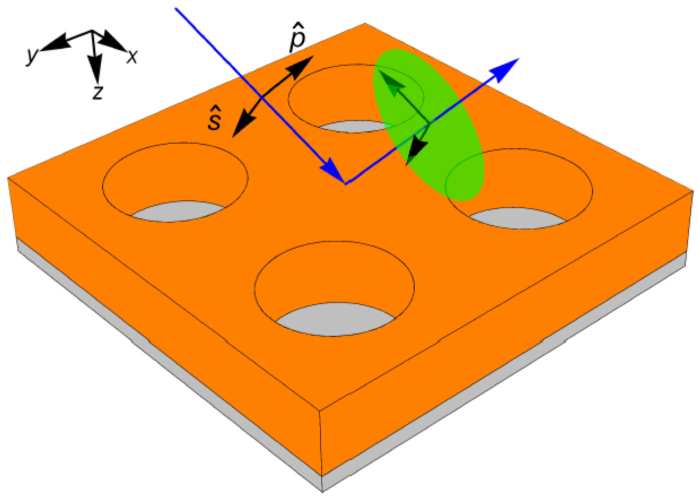

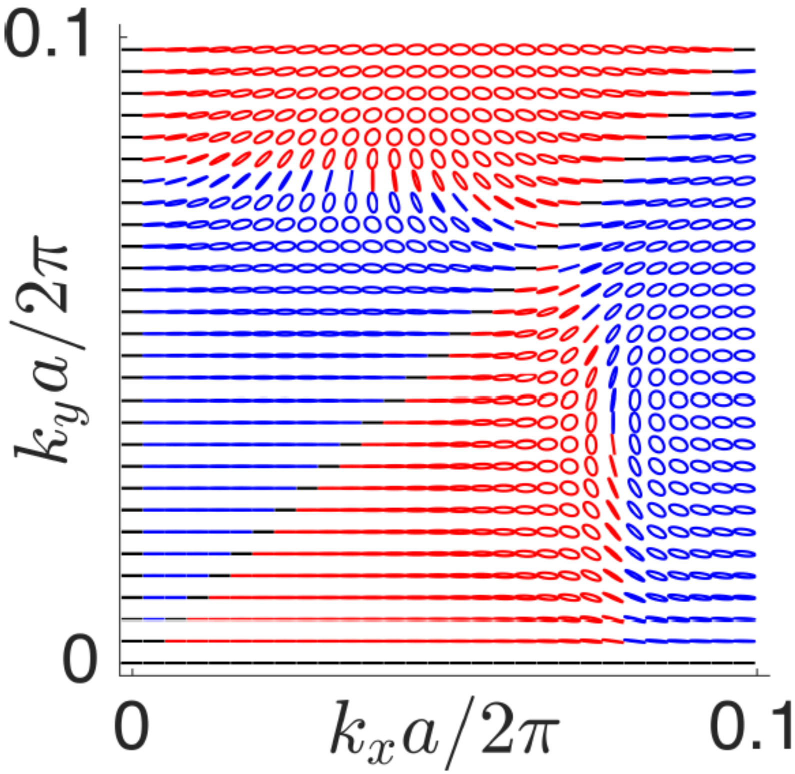

- Assume s-polarized incident light
- At a given frequency, by vary the angle of incidence, arbitrary output polarization can be generated.
- Such arbitrary polarization conversion is in fact topological, and can occur over large ranges of frequencies

Y. Guo, M. Xiao, Y. Zhou and S. Fan, Advanced Optical Materials art. No. 1801453 (2019)

Summary

Energy technology | Information technology | Fundamental aspects

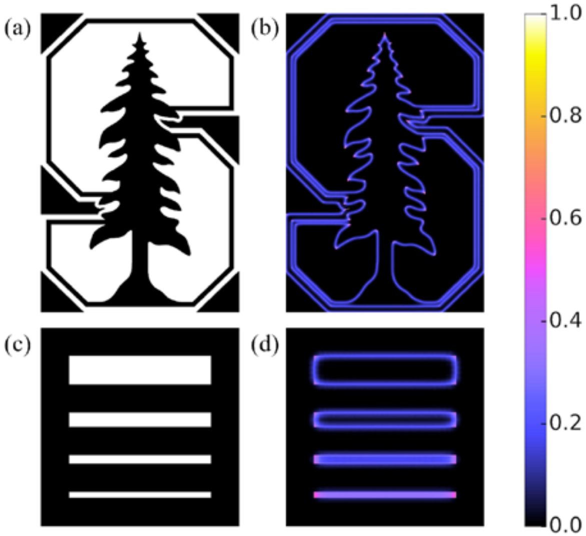

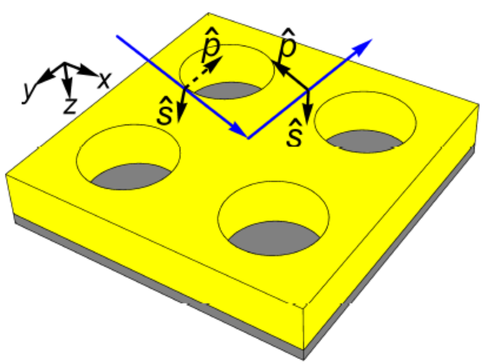

Radiative cooling | Image processing | Topology